

AD-A033 103

AIR FORCE MATERIALS LAB WRIGHT-PATTERSON AFB OHIO  
ANTIREFLECTION COATINGS FOR CALCIUM FLUORIDE LASER WINDOWS FOR --ETC(U)  
SEP 76 M C OHMER

F/G 20/5

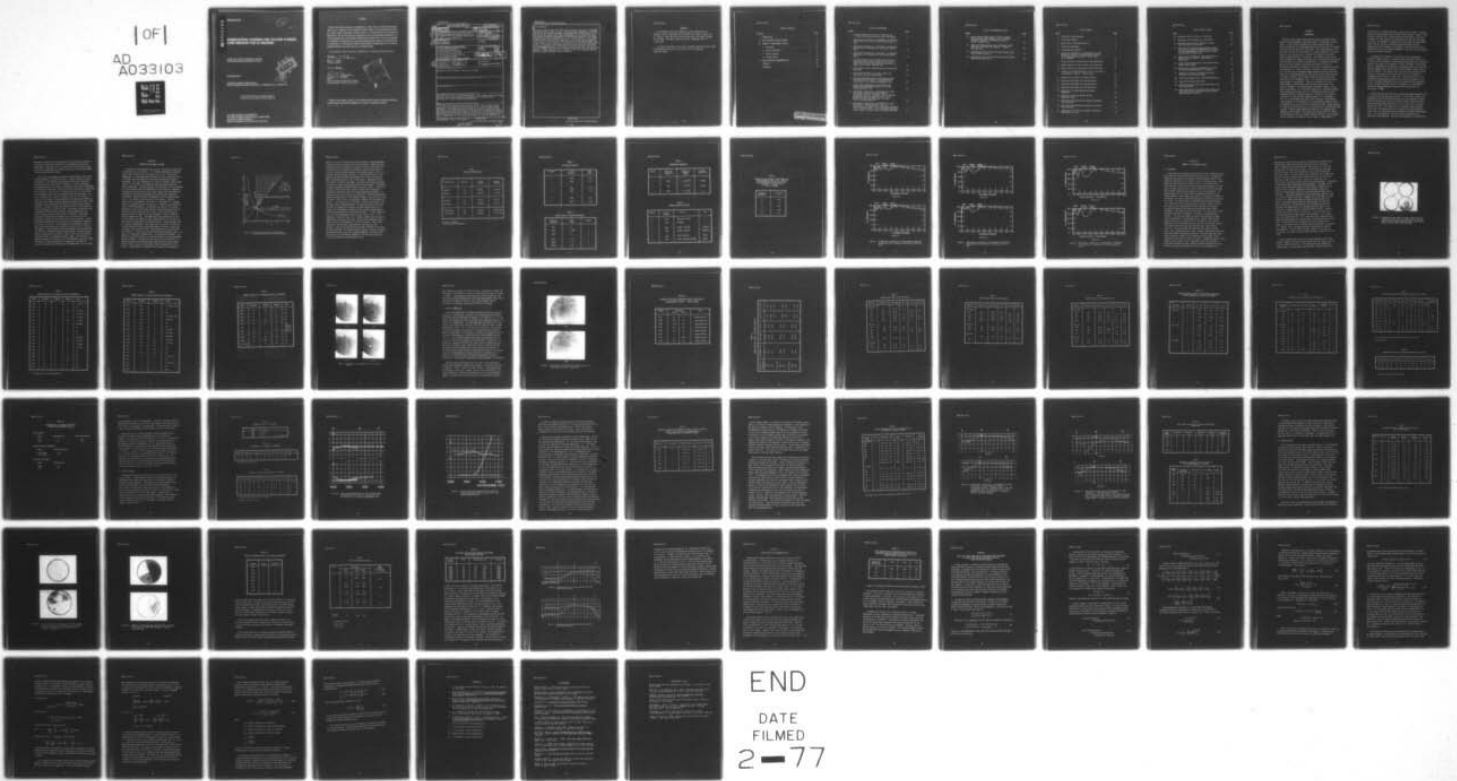
UNCLASSIFIED

AFML-TR-76-103

NL

| OF |

AD  
A033103



END

DATE  
FILMED  
2-77

ADA 033103

AFML-TR-76-103

12

B.S.

# ANTIREFLECTION COATINGS FOR CALCIUM FLUORIDE LASER WINDOWS FOR 5.3 MICRONS

LASER AND OPTICAL MATERIALS BRANCH  
ELECTROMAGNETIC MATERIALS DIVISION

D D C  
RECEIVED  
DEC 7 1976  
C

SEPTEMBER 1976

TECHNICAL REPORT AFML-TR-76-103  
FINAL TECHNICAL REPORT FOR PERIOD 1 OCTOBER 1974 to 1 MARCH 1976

Approved for public release; distribution unlimited

AIR FORCE MATERIALS LABORATORY  
AIR FORCE WRIGHT AERONAUTICAL LABORATORIES  
AIR FORCE SYSTEMS COMMAND  
WRIGHT-PATTERSON AIR FORCE BASE, OHIO 45433

NOTICE

When Government drawings, specifications, or other data are used for any purpose other than in connection with a definitely related Government procurement operation, the United States Government thereby incurs no responsibility nor any obligation whatsoever; and the fact that the government may have formulated, furnished, or in any way supplied the said drawings, specifications, or other data, is not to be regarded by implication or otherwise as in any manner licensing the holder or any other person or corporation, or conveying any rights or permission to manufacture, use, or sell any patented invention that may in any way be related thereto.

This technical report has been reviewed and is approved for publication.

*Melvin C. Ohmer*

MELVIN C. OHMER  
Project Engineer

FOR THE COMMANDER

*W D D Frederick*

WILLIAM G. D. FREDERICK  
Chief  
Laser and Optical Materials Branch  
Electromagnetic Materials Division

ACCESSION for

W/S	White Section	<input checked="" type="checkbox"/>
P.O.	B.M. Section	<input type="checkbox"/>
Doc		
BY	DIS. RIGHTS/AVAILABILITY CODES	
DATE	CLASS. CONTROL	

A

Copies of this report should not be returned unless return is required by security considerations, contractual obligations, or notice on a specific document.

UNCLASSIFIED

SECURITY CLASSIFICATION OF THIS PAGE (When Data Entered)

REPORT DOCUMENTATION PAGE		READ INSTRUCTIONS BEFORE COMPLETING FORM	
1. REPORT NUMBER AFML-TR-76-103	2. GOVT ACCESSION NO.	3. RESIDENTIAL CATALOG NUMBER Fiscal	
4. TITLE (and Subtitle) ANTIREFLECTION COATINGS FOR CALCIUM FLUORIDE LASER WINDOWS FOR 5.3 MICRONS,		5. TYPE OF REPORT & PERIOD COVERED Technical Report, 1 Oct 74 - 1 Mar 76	
6. AUTHOR(s) Melvin C. Ohmer		7. PERFORMING ORG. REPORT NUMBER	
		8. CONTRACT OR GRANT NUMBER(s) 73710156	
9. PERFORMING ORGANIZATION NAME AND ADDRESS Air Force Materials Laboratory (LPO) Air Force Systems Command Wright-Patterson AFB, OH 45433		10. PROGRAM ELEMENT, PROJECT, TASK AREA & WORK UNIT NUMBERS 62102F 73710156	(12)
11. CONTROLLING OFFICE NAME AND ADDRESS Air Force Materials Laboratory (LPO) Air Force Systems Command Wright-Patterson Air Force Base, OH 45433		12. REPORT DATE September 1976	75 p.
		13. NUMBER OF PAGES 75	
14. MONITORING AGENCY NAME & ADDRESS (if different from Controlling Office) (16) 7371 (17) 01		15. SECURITY CLASS. (of this report) Unclassified	
		15a. DECLASSIFICATION/DOWNGRADING SCHEDULE	
16. DISTRIBUTION STATEMENT (of this Report) Approved for public release; distribution unlimited.			
17. DISTRIBUTION STATEMENT (of the abstract entered in Block 20, if different from Report)			
18. SUPPLEMENTARY NOTES			
19. KEY WORDS (Continue on reverse side if necessary and identify by block number) antireflection coatings, carbon monoxide lasers, laser windows, optical coatings, infrared, alkaline earth fluorides, absorption, lead fluoride, thorium tetrafluoride, calcium fluoride, barium fluoride.			
20. ABSTRACT (Continue on reverse side if necessary and identify by block number) Four distinct antireflection (AR) coatings and half-wave coatings of their constituent coating materials were evaluated for 5.3 microns on CaF <sub>2</sub> and BaF <sub>2</sub> substrates. The coating materials were lead and strontium fluoride, thorium tetrafluoride, and zirconium dioxide. The coatings were evaluated with regard to absorption, peak transmission, bandwidth, residual strain, and adhesion. A PbF <sub>2</sub> / ThF <sub>4</sub> AR design had an absorption per surface less than .05%. The absorption of ZrO <sub>2</sub> is excessive at 5.3. All AR designs passed the scotch tape adhesion test.			

012320

1/3

UNCLASSIFIED

SECURITY CLASSIFICATION OF THIS PAGE(When Data Entered)

Block 20 (Contd)

The index of  $\text{SrF}_2$  in thin film form is lower than the bulk value. In half-wave coatings of  $\text{SrF}_2$  an index as low as 1.22 was observed. Bandwidths of three AR designs were 0.5 microns or greater. Absorptions of half-wave coatings at 1.06 and 3.8 microns indicate that further development will be required for these wavelengths. Absorption measurements for the  $\text{PbF}_2/\text{ThF}_4$  design for  $\text{CaF}_2$  windows coated on both sides are reported for 5.3, 3.8, and 2.8 microns. The windows absorbed 0.04%, 0.2%, and 0.5%, respectively. Some designs were plagued with stress induced birefringence in the visible which did not adversely affect the transmission in the IR. The  $\text{PbF}_2$ ,  $\text{ThF}_4$ , and  $\text{ZrO}_2$  coatings did not show residual strain. The absorption measurements obtained on three different calorimeters are compared. Expressions for equivalent or Herpin three-layer films for the case of arbitrary equivalent index and phase thickness are also contained in the Appendix. These expressions are an extension of the work of Epstein and they are not presently available from the literature.

UNCLASSIFIED

SECURITY CLASSIFICATION OF THIS PAGE(When Data Entered)

AFML-TR-76-103

FOREWORD

This technical report was prepared by the Air Force Materials Laboratory under Inhouse Work Unit 73710156, Task 737101, Project 7371. Dr. Melvin C. Ohmer was the principle investigator and project engineer for 73710156. The report covers the period 1 September 1974 to 1 March 1976.

The work was performed in the Laser and Optical Materials Branch (LPO), Electromagnetic Materials Division (LP), Air Force Materials Laboratory (AFML).

TABLE OF CONTENTS

SECTION	PAGE
I INTRODUCTION	1
II ANTIREFLECTION COATING DESIGNS	4
III SUMMARY OF EXPERIMENTAL RESULTS	14
1. Substrates	14
2. Optical Absorption	21
3. Optical Spectra	32
4. Coating Quality	43
IV CONCLUSIONS AND RECOMMENDATIONS	52
APPENDIX	54
REFERENCES	63

PROCEEDING USE BLANK NOT FILMED

## LIST OF ILLUSTRATIONS

FIGURE	PAGE
1. Schuster Diagram for $\text{CaF}_2$ for 5.3 Microns; the X's Indicate Coatings which Have Been Investigated	5
2. Theoretical Transmission vs Wavelength for $\text{PbF}_2/\text{ThF}_4$ AR Coatings for 5.3 Microns; 2a for $\text{CaF}_2$ and 2b for $\text{BaF}_2$	11
3. Theoretical Transmission vs Wavelength for $\text{PbF}_2/\text{SrF}_2$ AR Coating for 5.3 Microns; 3a for $\text{CaF}_2$ and 3b for $\text{BaF}_2$	12
4. Theoretical Transmission vs Wavelength for $\text{ZrO}_2/\text{ThF}_4$ AR Coating for 5.3 Microns; 4a for $\text{CaF}_2$ and 4b for $\text{BaF}_2$	13
5. Crossed-Polarizer Shot of Single Crystal and Polycrystalline $\text{CaF}_2$ ; Single Crystals on Top (Left to Right 1163 and 1152), Polycrystalline Substrates on Bottom (Left to Right 1079 and 1078)	16
6. Total Optical Figure (Twyman-Green) of Polished $\text{CaF}_2$ Substrates	20
7. Bulk Optical Uniformity of Single Crystal and Polycrystalline $\text{CaF}_2$ , Twyman-Green	22
8. Single Surface Reflectance for $\text{CaF}_2$ Witness Wedge for Sample 1087 for Side R1. Data Obtained by Perkin-Elmer on P-E 180 Spectrophotometer (5X)	34
9. Single Surface Reflectance for AR Coated $\text{CaF}_2$ Witness Piece Obtained by Valpey on a P-E 180 Spectrophotometer (10X)	35
10. Experimental Transmission vs Wavelength (P-E 180) for Design 1 (10a) and Design 2 (10b) on Polycrystalline $\text{CaF}_2$ . The Upper Trace is the 100% Calibration Line. The middle Trace is for the Quadrant AR Coated on Both Sides. The Lower Trace is the Bare Substrate	40
11. Experimental Transmission vs Wavelength (P-E 180) for Design 3 (11a) and Design 4 (11b) on Polytran $\text{CaF}_2$ . The Upper Trace is the 100% Calibration Line. The Middle Trace is for the Quadrant AR Coated on Both Sides. The Lower Trace is the Bare Substrate	41

## LIST OF ILLUSTRATIONS (Contd)

FIGURE	PAGE
12. Strain Induced Birefringence in Visible Crossed-Polarizer Shot, Before Coating (Top), and After AR Coating (Bottom). The Quadrant Format Is Visible. (Sample 1173)	45
13. Sample of Streaky Residual Strain Patterns, Sample 1076 (Top) and Sample 1068 (Bottom). Crossed-Polarizer Shot	46
14. Transmission Scans for $ZrO_2$ Half-wave Coating (1070). Beam Incident on Side R1	50
15. Transmission Scans for $ZrO_2$ Half-wave Coating (1070). Beam Incident on Side R2	50

## LIST OF TABLES

TABLE	PAGE
1. Theoretical Coating Designs	7
2. Film Design Indices	8
3. Design Index of Substrate Material	8
4. Evaporation Parameters	9
5. Coating Material Supplier	9
6. Theoretical Reflectance vs Wavelength for a $\text{CaF}_2$ Window for $\text{PbF}_2/\text{ThF}_4$ Quarter-Quarter Coating for the Respective Indices of 1.73 and 1.49 for 5.3 Microns	10
7. Sample Identity of Polycrystalline $\text{CaF}_2$ Substrates	17
8. Sample Identity of Single Crystal $\text{CaF}_2$ Substrates	18
9. Sample Identity of Polycrystalline $\text{BaF}_2$ Substrates	19
10. Flatness of Polished Substrates Given in Fractions of a Wavelength at 5461 Å. (Peak to Peak)	23
11. Absorption Data (UDRI) for Coating Design 1	24
12. Absorption Data (UDRI) for Coating Design 2	25
13. Absorption Data (UDRI) for Coating Design 3	26
14. Absorption Data (UDRI) for Coating Design 4	27
15. Comparison of Coating Designs by Average Absorption	28
16. Comparison of Coating Designs by Best Absorption Value	29
17. Absorption Data Obtained on Northrop Calorimeter for 5.3 Microns	30
18. Absorption Data Obtained on Raytheon Calorimeter for 5.3 Microns	30
19. Comparison of 5.3 Micron Calorimeter Absorption Measurements on $\text{CaF}_2$	31

## LIST OF TABLES (Contd)

TABLE	PAGE
20. Absorption (AFIT) of CaF <sub>2</sub> at 1.06 Microns	33
21. Absorption of $\lambda/2$ Coatings at 1.06 Microns	33
22. Absorption (University of Alabama) of Single Layer Coatings at 3.8 Microns	33
23. Comparison of Transmission Measurements on Bare CaF <sub>2</sub> and BaF <sub>2</sub> Substrates Obtained on Perkin-Elmer 180 Spectrophotometers by Perkin-Elmer, Valpey, and University of Miami, Ohio	37
24. Comparison of Transmission, Peak Wavelength and Bandwidth for AR coatings. (University of Miami, Ohio)	39
25. Single Surface Reflectivity of AR Coated Witness Wedges (Perkin-Elmer)	42
26. Comparison of Transmission Measured on Various P-E 180 Spectrophotometers at 5.3 Microns	42
27. Comparison of Optical Thickness and Physical Thickness for Half-wave Coatings	44
28. Scotch Tape Adhesion Test of AR Coated Substrates	47
29. Topple Test Adhesion Data (UDRI)	48
30. Half-wave Coating Single Surface Reflectance from Perkin-Elmer Data	49
31. Total Absorption for Oriented Single Crystal CaF <sub>2</sub> Substrates Coated on Both Sides with PbF <sub>2</sub> /ThF <sub>4</sub> Quarter-Quarter AR Coating	53

## SECTION I

## INTRODUCTION

During the past several years there has been a substantial effort devoted to the development of physical windows for high power infrared lasers. Initial efforts concentrated on polycrystalline CVD zinc selenide (ZnSe) and hot forged doped potassium chloride (KCl) for windows for carbon dioxide lasers at 10.6 microns. The present emphasis of the effort has shifted to the development of physical windows for the carbon monoxide laser operating near 5 microns and the deuterium fluoride chemical laser operating at 3.8 microns. The materials which are the prime candidates for windows for these lasers are polycrystalline calcium fluoride ( $\text{CaF}_2$ ) and strontium fluoride ( $\text{SrF}_2$ ). The general performance goal for physical windows is that the total optical loss due to absorption, reflection, and scatter be less than 0.1% where the loss due to absorption is as small as possible. Because of Fresnel reflection loss, arising from an impedance mismatch between dissimilar media and amounting to approximately 30% for ZnSe and 6% for the other materials for normal incidence, special measures must be taken to reduce the reflectivity to an acceptable level. For a polarized beam a Brewster angle window is a possibility. There is no reflection loss for a beam incident at the Brewster angle and polarized parallel to the plane of incidence. For these materials, Brewster's angle is of the order of 60 degrees. For a given beam diameter (D) a 60-degree Brewster angle window has twice the area of a corresponding window at normal incidence and has an effective length of  $nD$  where  $n$  is the index of refraction. A typical normal window thickness is 1-2 centimeters. For a 25 cm beam diameter the ratio of the thickness of the Brewster angle window to a 2 cm thickness of the corresponding window at normal incidence would be 18 for the case of  $\text{CaF}_2$ , 64 for ZnSe. Another approach to reducing the reflection loss is the utilization of antireflection (AR) coatings. These coatings perform the function of an impedance match between dissimilar media. The simplest AR coating which will reduce the reflectance to zero for normal incidence consists of a quarter-wave optical thickness of a material with an index of  $\sqrt{n_1 n_2}$  where  $n_1$  is

the index of the incident media and  $n_2$  that of the exit media. Usually, a material which possesses such an index cannot be found. However, there are many realizable two or three-layer AR coating designs. Analytical expressions for the required film thicknesses for two-layer AR coatings are given in the Appendix. Expressions for equivalent or Herpin three-layer films for the case of arbitrary equivalent index and phase thickness are also contained in the Appendix. These expressions are an extension of the work of Epstein (Reference 1) and they are not presently available from the literature.

The problem of AR coatings is a particular case of the generic problem of energy transfer. As another example, consider the case of an elastic collision between a moving spherical mass ( $M_1$ ) and a stationary spherical mass ( $M_2$ ) for the geometry of normal incidence. Total energy transfer is obtained by positioning an intermediate sphere with mass ( $M_I$ ) equal to  $\sqrt{M_1 M_2}$  between the two masses. (Golly Batman, shades of wave-particle duality). The special case of  $M_1$  equal to  $M_2$  accounts for the behavior of the executive passifier which consists of a number of suspended spherical masses of equal size. For the familiar case of a loudspeaker, maximum energy transfer occurs where the diameter of the horn is increasing exponentially with the distance from the diaphragm. For this situation the mass ( $M_I$ ) of the pancake of air intermediate between two adjacent pancakes of masses  $M_1$  and  $M_2$  satisfies the relation  $M_I = \sqrt{M_1 M_2}$ .

An excellent two-layer AR coating has been developed (References 2,3) for ZnSe for 10.6 microns which consists of a first layer (nearest the substrate) of thorium tetrafluoride ( $\text{ThF}_4$ ) and a second layer of ZnSe, which has an absorption loss per surface of 0.03%. A promising three-layer AR coating design consisting of a first layer of TlI, a second layer of KCl, and a third layer of TlI is presently being developed for KCl for 10.6 microns which has an absorption loss per surface of 0.05%. These low absorptions were only obtained by extensive development work. It is not unusual for one of the coating materials to be identical to the substrate. The role of the coatings is to control the

amplitude and phase of the reflections from the coating and substrate interfaces such that total reflection is eliminated by destructive interference. When the index of refraction of the substrate is appropriate for incorporation as a coating material into the coating design the design may have fewer layers.

Very little is presently known about the performance of AR coated fluoride windows for 3.8 and 5.3 microns. However, there are reasons for optimism. The candidate window materials are hard, relatively insoluble, and have a low index of refraction. There are many more coating materials that are highly transparent at the shorter wavelengths. The absorption coefficient of films at 5.3 and 3.8 microns is respectively in the range of  $1 \text{ cm}^{-1}$  and  $4 \text{ cm}^{-1}$  compared to  $10 \text{ cm}^{-1}$  at 10.6 microns. Film thicknesses required for AR coatings scale with wavelength. As a result, coatings for 3.8 and 5.3 microns are 1/3 to 1/2 as thick as those for 10.6 microns. Characterization of the optical performance of high power laser windows requires measurement capabilities such as laser calorimetry which are beyond those available to most coating vendors. Therefore, a program to assess the state-of-the-art of AR coatings for fluoride windows was initiated by AFML. The approach consisted of the procurement of AR coated two-inch  $\text{CaF}_2$  and  $\text{BaF}_2$  samples from four vendors, Hughes, Northrop, Perkin-Elmer, and Valpey. Each vendor delivered 12 samples which included five single crystal and five polycrystalline  $\text{CaF}_2$  and two polycrystalline  $\text{BaF}_2$  substrates. Design philosophy, nonproprietary coating designs, and deposition parameters are given in Section II. These samples were evaluated with regard to absorption, peak transmission, bandwidth, residual strain, flatness, and adhesion. These evaluations were performed by the coating vendors, the University of Dayton Research Institute (UDRI), Raytheon Research Division, the University of Miami of Ohio, the Air Force Institute of Technology (AFIT), the Honeywell Ceramics Center, the University of Alabama at Huntsville, and by the Air Force Materials Laboratory (AFML). The results of these measurements are summarized in Section III. Section IV contains the conclusions and recommendations for this study.

SECTION II  
ANTIREFLECTION COATING DESIGNS

In contrast to the output of the CO<sub>2</sub> laser, the output of the CO and the chemical laser is multiline. M. L. Bhaumik (Reference 5) obtained typical spectra output from a particular CO laser as a function gas temperature. At room temperature the spectral output ranged from 5.3 to 5.7 microns with the energy fairly evenly distributed with regard to wavelength. For a wall temperature of -183°C the spectral output ranged from 5.1 to 5.5 microns with energy distribution skewed toward the shorter wavelength. Strictly speaking, the acceptability of the bandwidth of a coating design should be determined by calculating the integrated reflectance utilizing the particular laser spectra that the window will encounter and the design wavelength which minimizes the integrated reflectance. Roughly speaking, the bandwidth of the AR coating should be 0.4 - 0.5 microns for the CO and DF laser windows. Excessive specification of bandwidth for the case of a beam with  $E(\lambda) = \text{constant}$ , results in a complex coating of many layers. Therefore, care should be taken in defining bandwidth. Fortunately, the index of the fluoride substrates is very low and there are many coating designs which utilize materials, both of which have low indices. For this situation even designs of only two layers are fairly broadband. Figure 1 shows the Schuster diagram for CaF<sub>2</sub>. The numbering/listing convention for films in this report is to number/list the coating materials in the order in which they are deposited on the window substrate. The design wavelength for coatings investigated in this report was 5.3 microns. Any pair of indices selected from the cross-hatched region of Figure 1 may be used to produce a two-layer AR coating. Coordinates which also satisfy the relationship  $n_1 = n_2 \sqrt{n_s}$  have a quarter-wave optical-thickness ( $nd/\lambda = .25$  where  $d$  is the physical thickness and  $\lambda$  is the design wavelength). The physically realizable designs are confined to Region 1 and the broadband designs in Region 1 are those with the value of  $n_1$  well below 2.0. A CeF<sub>3</sub>/MgF<sub>2</sub> quarter-quarter design where the design indices were respectively 1.59 and 1.33 was investigated by Hughes (Reference 6) for 5.3 microns. Unfortunately, the absorption was excessive and absorption

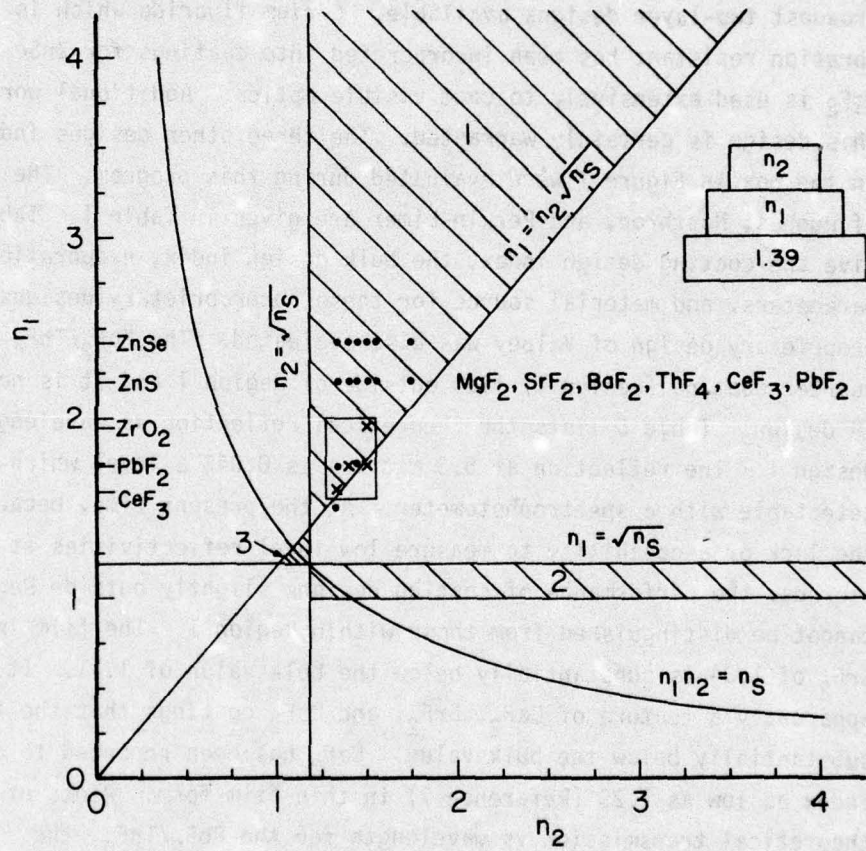


Figure 1. Schuster Diagram for  $\text{CaF}_2$  for 5.3 Microns; the X's Indicate Coatings which Have Been Investigated

bands at 2.9 and 6.1 microns were clearly visible in spectrophotometer transmission scans for AR and single layer coatings. These bands were attributed to the incorporation of water into the film which may have occurred during film growth or was present in the starting material. This result was unfortunate because the  $\text{CeF}_3/\text{MgF}_2$  design is one of the broadest two-layer designs available. Cerium fluoride which is very abrasion resistant has been incorporated into coatings for ZnSe and  $\text{MgF}_2$  is used extensively to coat visible optics. Additional work on this design is certainly warranted. The three other designs indicated in the box in Figure 1 were evaluated during this program. The designs of Hughes, Northrop, and Perkin-Elmer are given in Table 1. Tables 2-5 give the coating design index, the bulk design index, evaporation parameters, and material source for these nonproprietary designs. A proprietary design of Valpey was also evaluated. The  $\text{PbF}_2/\text{ThF}_4$  quarter-quarter coating (design 1) lies outside of Region 1 and it is not a true AR design. Table 6 lists the theoretical reflection vs wavelength for Design 1. The reflection at 5.3 microns is 0.04% a level which is not detectable with a spectrophotometer. At the present time, because of the lack of a capability to measure low level reflectivities at 5.3 microns, the performance of coating designs slightly outside Region 1 cannot be distinguished from those within Region 1. The film index for  $\text{SrF}_2$  of 1.34 is substantially below the bulk value of 1.41. It is apparently a feature of  $\text{CaF}_2$ ,  $\text{SrF}_2$ , and  $\text{BaF}_2$  coatings that the index is substantially below the bulk value.  $\text{CaF}_2$  has been reported to have an index as low as 1.29 (Reference 7) in thin film form. Plots of the theoretical transmission vs wavelength for the  $\text{PbF}_2/\text{ThF}_4$ , the  $\text{PbF}_2/\text{SrF}_2$ , and the  $\text{ZrO}_2/\text{ThF}_4$  designs are given in Figures 2-4 for  $\text{CaF}_2$  and  $\text{BaF}_2$  substrates. As expected from the Schuster diagram, the design incorporating the  $\text{ZrO}_2$  has the narrowest bandwidth. The design incorporating  $\text{SrF}_2$  has the broadest bandwidth. The  $\text{PbF}_2/\text{ThF}_4$  design for  $\text{CaF}_2$  was not modified when deposited on  $\text{BaF}_2$ .

TABLE 1  
THEORETICAL COATING DESIGNS

Vendor/Design**	Substrate	Film* Material	Optical Thickness
Hughes/1	CaF <sub>2</sub>	PbF <sub>2</sub> /SrF <sub>2</sub>	.113λ/.308λ
Hughes/1	BaF <sub>2</sub>	PbF <sub>2</sub> /SrF <sub>2</sub>	.142λ/.282λ
Northrop/2	CaF <sub>2</sub>	PbF <sub>2</sub> /ThF <sub>4</sub>	.25λ/.25λ
Northrop/2	BaF <sub>2</sub>	PbF <sub>2</sub> /ThF <sub>4</sub>	.25λ.25λ
Perkin-Elmer/3	CaF <sub>2</sub>	ZrO <sub>2</sub> /ThF <sub>4</sub>	.1135λ/.3259λ
Perkin-Elmer/3	BaF <sub>2</sub>	ZrO <sub>2</sub> /ThF <sub>4</sub>	.1234λ/.3156λ

\* In order of deposition  
\*\*The Valpey design was designated 4

TABLE 2  
FILM DESIGN INDICES

Design	Film Material	Film Index
1	SrF <sub>2</sub>	1.34
1	PbF <sub>2</sub>	1.71
2	ThF <sub>4</sub>	1.49
2	PbF <sub>2</sub>	1.73
3	ThF <sub>4</sub>	1.49
3	ZrO <sub>2</sub>	1.95

TABLE 3  
DESIGN INDEX OF SUBSTRATE MATERIAL

Substrate Material	Bulk Index	Design
CaF <sub>2</sub>	1.4	1
CaF <sub>2</sub>	1.3999	2
CaF <sub>2</sub>	1.4	3
BaF <sub>2</sub>	1.45	1
BaF <sub>2</sub>	1.45	2
BaF <sub>2</sub>	1.45	3

TABLE 4  
EVAPORATION PARAMETERS

Design	Substrate Temperature (°C)	Deposition Pressure (Torr)	Source Temperature
3	250°	$2 \times 10^{-6}$	e-beam
2	200°	$5 \times 10^{-6}$	e-beam
1	200°	$1 \times 10^{-6}$	—

TABLE 5  
COATING MATERIAL SUPPLIER

Design	Film Material	Source	Form
1	SrF <sub>2</sub>	RAP grown at HRL	—
1	PbF <sub>2</sub>	Harshaw	—
2	PbF <sub>2</sub>	Balzers (99.9%)	granular
2	ThF <sub>4</sub>	Balzers (99.9%)	granular
3	ZrO <sub>2</sub>	Cerac (99.7%)	chunk
3	ThF <sub>4</sub>	Cerac (TS-106; 99.99%)	chunk

TABLE 6

THEORETICAL REFLECTANCE VS WAVELENGTH FOR  
A  $\text{CaF}_2$  WINDOW FOR  $\text{PbF}_2/\text{ThF}_4$ . QUARTER-  
QUARTER COATING FOR THE RESPECTIVE  
INDICES OF 1.73 AND 1.49  
FOR 5.3 MICRONS

Wavelength (microns)	Reflection %
5.0	.18%
5.1	.11
5.2	.04
5.3	.04
5.4	.08

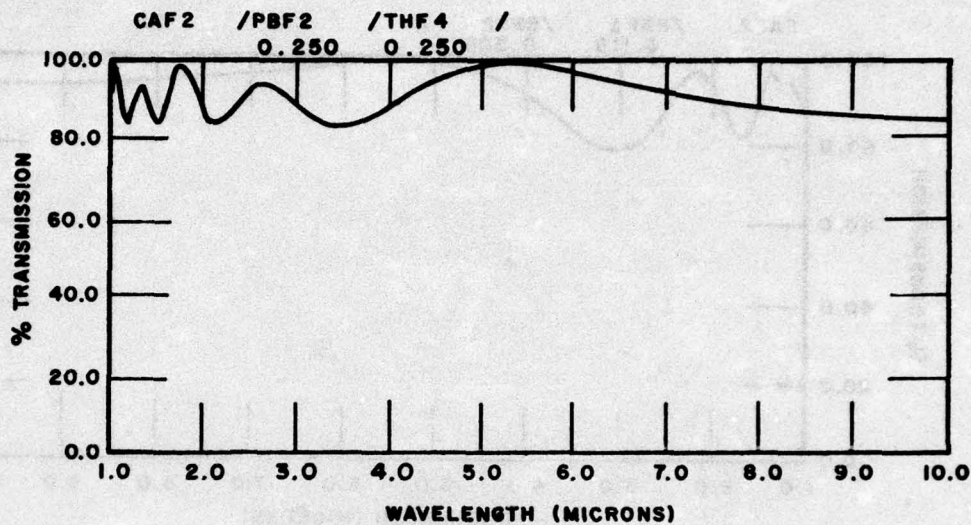


Figure 2a

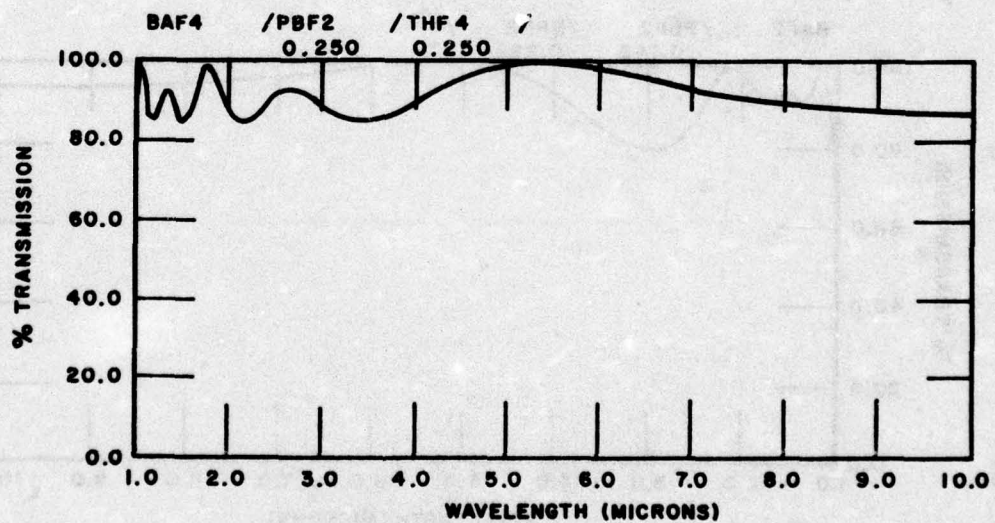


Figure 2b

Figure 2. Theoretical Transmission vs Wavelength for PbF<sub>2</sub>/ThF<sub>4</sub> AR Coatings for 5.3 Microns; 2a for CaF<sub>2</sub> and 2b for BaF<sub>2</sub>

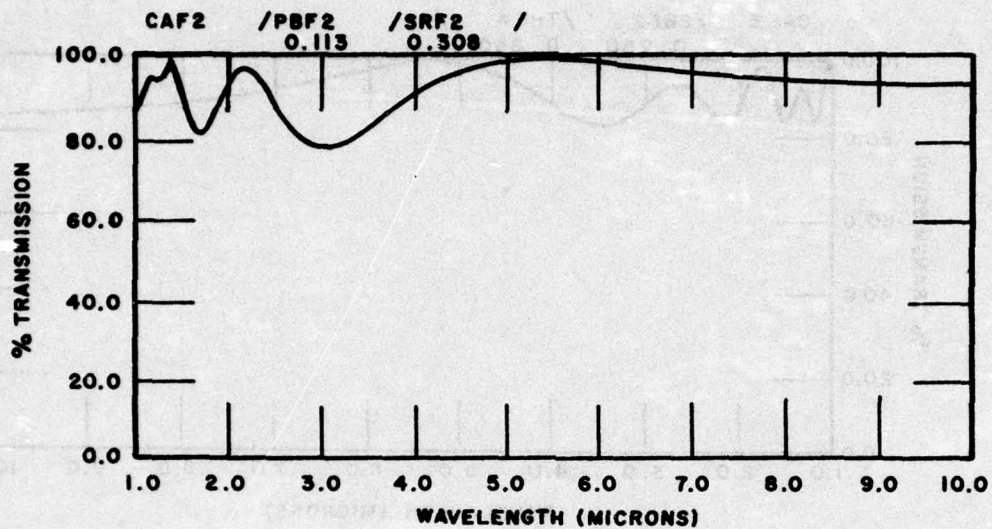


Figure 3a

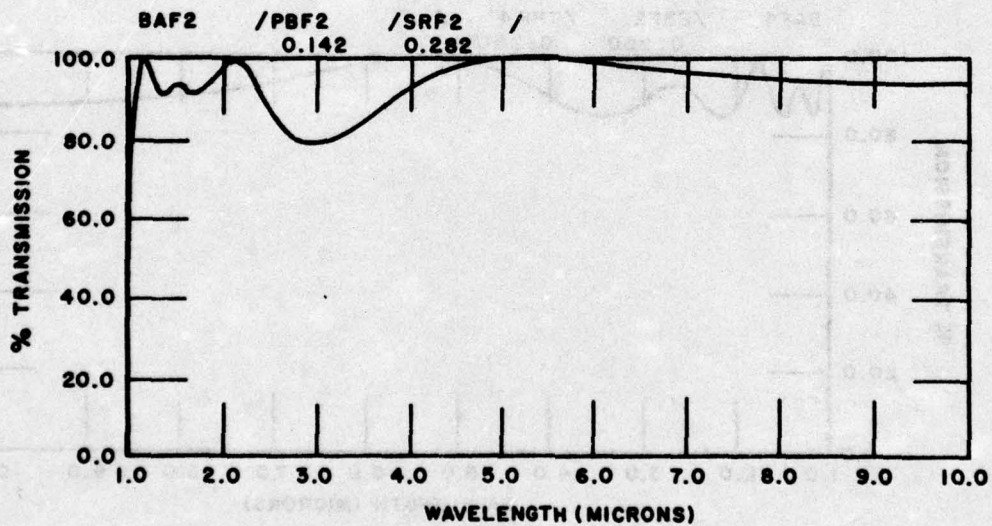


Figure 3b

Figure 3. Theoretical Transmission vs Wavelength for PbF<sub>2</sub>/SrF<sub>2</sub> AR Coating for 5.3 Microns; 3a for CaF<sub>2</sub> and 3b for BaF<sub>2</sub>

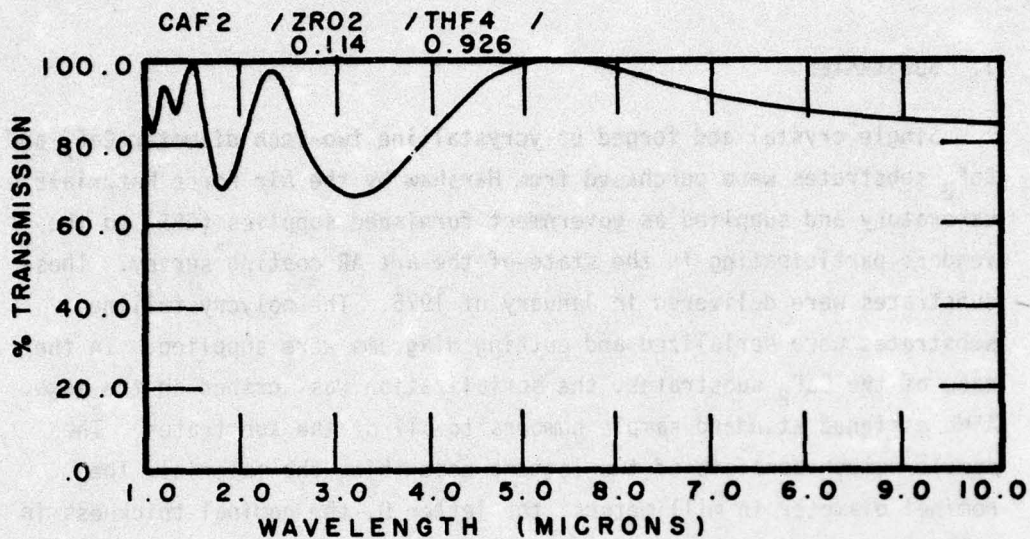


Figure 4a

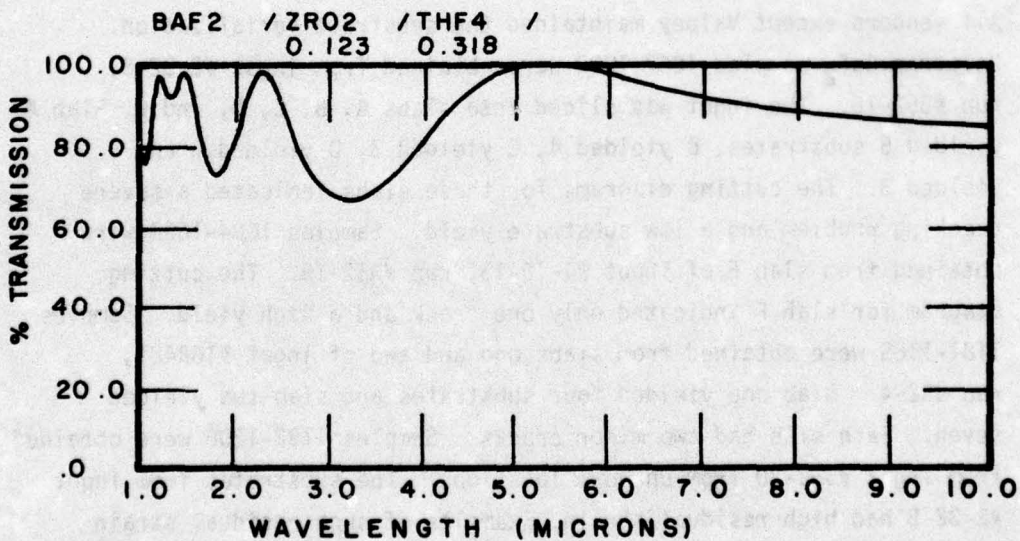


Figure 4b

Figure 4. Theoretical Transmission vs Wavelength for ZrO<sub>2</sub>/ThF<sub>4</sub> AR Coating for 5.3 Microns; 4a for CaF<sub>2</sub> and 4b for BaF<sub>2</sub>

SECTION III  
SUMMARY OF EXPERIMENTAL RESULTS

## 1. SUBSTRATES

Single crystal and forged polycrystalline two-inch diameter  $\text{CaF}_2$  and  $\text{BaF}_2$  substrates were purchased from Harshaw by the Air Force Materials Laboratory and supplied as government furnished supplies (GFS) to the vendors participating in the state-of-the-art AR coating survey. These substrates were delivered in January of 1975. The polycrystalline substrates were serialized and cutting diagrams were supplied. In the case of the  $\text{BaF}_2$  substrates, the serialization was scribed on the edge. AFML assigned standard sample numbers to all of the substrates. The sample number consists of two letters describing the material, the nominal diameter in millimeters, the letter D, the nominal thickness in millimeters, two letters describing the supplier followed by a dash and four digits. An example would be CF51D10HA-1067 which describes the first substrate for this program logged in by AFML as shown in Table 7. All vendors except Valpey maintained the substrate serialization. Polytran  $\text{CaF}_2$  samples 1067-1083 were obtained from ingot #2-32-8, run #352-16. The ingot was sliced into slabs A, B, C, D, and E. Slab A yielded 5 substrates, B yielded 4, C yielded 3, D yielded 3 and E yielded 3. The cutting diagrams for these slabs indicated a severe cracking problem and a low substrate yield. Samples 1084-1090 were obtained from slab F of ingot #1-16-13, run #352-18. The cutting diagram for slab F indicated only one crack and a high yield. Samples 1181-1189 were obtained from slabs one and two of ingot #16R421, run 452-4. Slab one yielded four substrates and slab two yielded seven. Each slab had two minor cracks. Samples 1192-1206 were obtained from ingot #352-20 from unknown locations. The substrates from ingot #2-32-8 had high residual strain. Examples of such residual strain (samples 1078 and 1079) are shown in Figure 5. Substrates from the other ingots had very little strain. Twenty-two forged  $\text{CaF}_2$  substrates delivered in November of 1975 to AFML by Harshaw had essentially zero residual strain so the substrates utilized in this program do not

AFML-TR-76-103

represent the state of the art material with regard to residual strain. Polytran  $\text{BaF}_2$  samples were obtained from three slabs cut from one ingot. Samples 1164-1170 were obtained from slab one, 1171-1175 from slab two and 1176-1180 from slab three. The Polytran  $\text{BaF}_2$  substrates had less residual strain than the Polytran  $\text{CaF}_2$  substrates obtained from ingot 2-32-8. No strain pattern was evident near the scribed area. Tables 7-9 give the various sample numbers describing the substrates, the coating vendor and the type of coating for respectively the Polytran  $\text{CaF}_2$ , the single crystal  $\text{CaF}_2$ , and the Polytran  $\text{BaF}_2$ . Traceability of the single crystal substrates was not possible. The single crystal substrates were optically superior to the Polytran. Comments such as cloudy in parts, crystal structure in parts, mottled, inclusions, internal cleavage planes, and stria were associated with the Polytran substrates. The cutting diagrams for the Polytran  $\text{BaF}_2$  indicates black floc and black specs in the slabs. Samples 1173, 1180, 1076, and 1084 had digs in as-received surfaces which were too deep to polish out. Several optically polished samples of polytran had a few scratches which exceeded 40. The Polytran  $\text{BaF}_2$  final thickness for polished substrates was approximately one millimeter less than that of  $\text{CaF}_2$  indicating a greater removal of material during polishing. Generally the  $\text{BaF}_2$  was visually inferior to the  $\text{CaF}_2$ . The grain size of the Polytran substrates was approximately one centimeter. All coatings were in the quadrant format. All of the Perkin-Elmer samples and the Hughes half-wave samples had fiducial marks indicating side one (S1) and (S2). The coating on S1 was deposited first for the Perkin-Elmer samples. Each Perkin-Elmer AR coated sample was produced in a separate run. However, their half-wave coatings of each type were produced simultaneously. For the Hughes half-wave coatings, S1 was  $\text{PbF}_2$  and S2 was  $\text{SrF}_2$ . All other half-wave samples had the same material on both sides.

Figure 6 depicts the total optical figure obtained by two of the vendors. Samples 1078 and 1079 are Polytran  $\text{CaF}_2$  and samples 1163 and 1152 are single crystal  $\text{CaF}_2$ . The interferograms were obtained at .6328 microns on a Twyman-Green interferometer. Sample 1078 has the

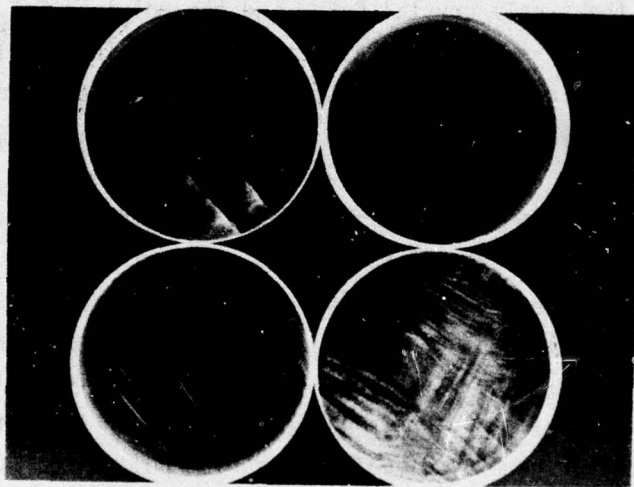


Figure 5. Crossed-Polarizer Shot of Single Crystal and Polycrystalline  $\text{CaF}_2$ ; Single Crystals on Top (Left to Right 1163 and 1152), Polycrystalline Substrates on Bottom (Left to Right 1079 and 1078)

TABLE 7  
 SAMPLE IDENTITY OF POLYCRYSTALLINE  $\text{CaF}_2$  SUBSTRATES

AFML#	HARSHAW#	VENDOR#	VENDOR	TYPE
1067	1*	1	V	$\lambda/2$ mat'1 1
1068	2*	2	V	AR
1070	5	5	P-E.	$\lambda/2$ $\text{ZrO}_2$
1071	6*	3	V	$\lambda/2$ mat'1 2
1072	7	7	N	$\lambda/2$ $\text{PbF}_2$
1073	8	8	P-E	$\lambda/2$ $\text{ThF}_4$
1074	9	9	H	Polished
1075	10	10	H	$\lambda/2$
1076	11	11	H	AR
1077	12	12	N	AR
1078	13*	4	V	Polished
1079	14	14	P-E	Polished
1081	16	16	N	Polished
1082	17	17	N	$\lambda/2$ $\text{ThF}_4$
1084	19	19	H	AR
1085	20	20	H	$\lambda/2$
1086	21	21	P-E	AR
1087	22	22	P-E	AR
1089	24	24	N	AR
1090	25*	5	V	AR

\* Identify with cutting diagram lost

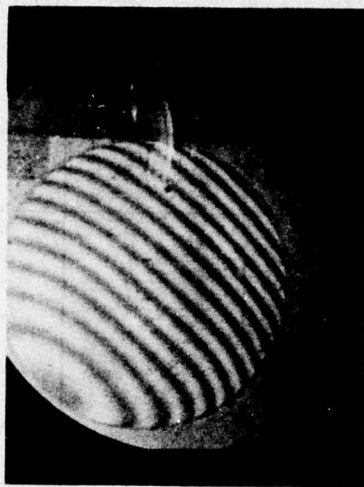
TABLE 8  
 SAMPLE IDENTITY OF SINGLE CRYSTAL  $\text{CaF}_2$  SUBSTRATES

AFML#	VENDOR#	VENDOR	TYPE
1134	1134	H	$\lambda/2$ $\text{PbF}_2$ , $\text{SrF}_2$
1135	1135	H	AR
1136	1136	H	AR
1137	1137	H	$\lambda/2$ $\text{PbF}_2$ , $\text{SrF}_2$
1138	1138	H	Polished
1144	1144	N	AR
1145	1145	N	AR
1146	1146	N	$\lambda/2$ $\text{PbF}_2$
1147	1147	N	$\lambda/2$ $\text{ThF}_4$
1148	1148	N	Polished
1149	145	P-E	$\lambda/2$ $\text{ZrO}_2$
1150	150	P-E	$\lambda/2$ $\text{ThF}_4$
1151	151	P-E	AR
1152	—	P-E	Bare
1153	153	P-E	AR
1159	1	V	$\lambda/2$ mat'1 2
1160	2	V	AR
1161	3	V	$\lambda/2$ mat'1 1
1162	4	V	AR
1163	5	V	Bare

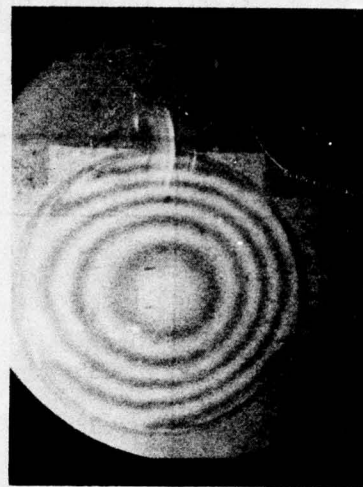
AFML-TR-76-103

TABLE 9  
SAMPLE IDENTITY OF POLYCRYSTALLINE BaF<sub>2</sub> SUBSTRATES

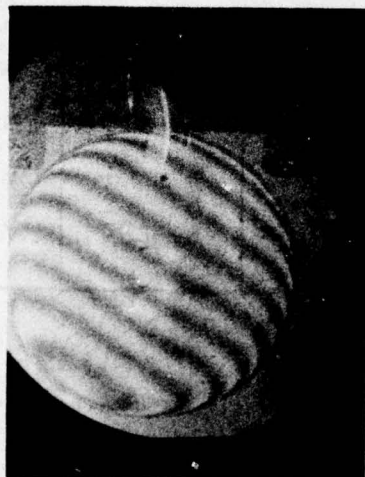
AFML#	HARSHAW#	VENDOR#	VENDOR	TYPE
1164	30	30	N	AR
1166	32	2	V	AR
1169	35	—	P-E	AR
1172	38	38	N	AR
1173	39	1173	H	AR
1174	40	—	P-E	Second Mailing
1176	45	—	P-E	Second Mailing
1177	46	1	V	AR
1178	47	42	P-E	AR
1180	52	1180	H	AR
xtal BaF <sub>2</sub>	—	A	P-E	AR



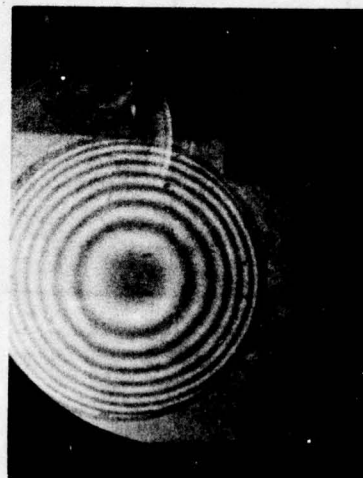
1078



1079



1163



1152

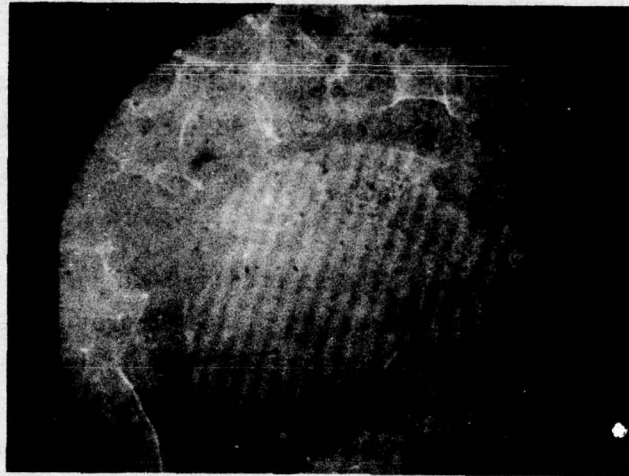
Figure 6. Total Optical Figure (Twyman-Green) of Polished  $\text{CaF}_2$  Substrates

best figure while samples 1079 and 1152 show a high degree of sphericity. Bulk optical uniformity for a single and polycrystalline sample is shown in Figure 7. The flatness of each side of the polished substrates was determined by using an optical flat and monochromatic green light (5461 Å). The results are given in Table 10. One  $\lambda$  peak to peak at 5461 Å corresponds to  $\lambda/10$  peak to peak and  $\lambda/27$  RMS at 5.3 microns.

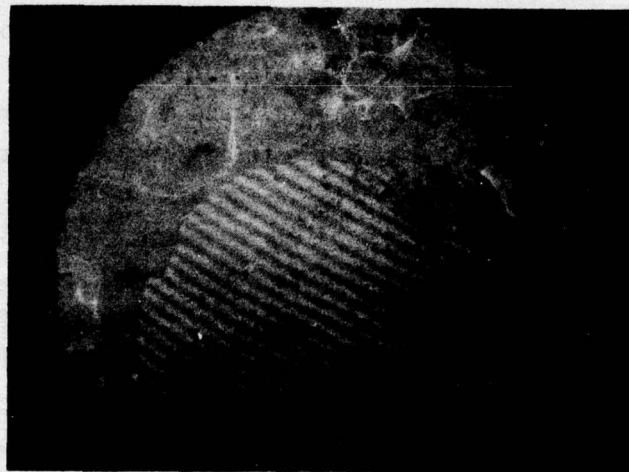
## 2. OPTICAL ABSORPTION

The initial measurement on samples produced during this program was absorption at 5.3 microns. The results of the absorption measurements obtained by UDRI are tabulated for Designs 1-4 in Tables 11-14. For the single side AR coating or the  $\lambda/2$  coatings, the coating was always on the side of the incident beam. The room temperature specific heat for  $\text{CaF}_2$  and  $\text{BaF}_2$  was respectively .895 J/gm-K and .405 J/gm-K and their indices respectively 1.40 and 1.45. The CO laser was cooled by a dry-ice bath. The transmitted power was measured by a Coherent Radiation Laboratory Model 201 power meter. In the tables,  $A_u$  refers to the absorption of an uncoated substrate and  $A_c$  to the absorption of the coated substrate ( $\Delta A = A_c - A_u$ ). Table 15 compares the average coating absorption per surface for the various designs for the three types of substrates. On the basis of absorption the  $\text{PbF}_2/\text{ThF}_4$  design with a coating absorption per surface of 0.02 - 0.04% is definitely superior. Table 16 compares the best value of absorption per surface for the various designs for the three types of substrates and it indicates that three of the designs occasionally approached or surpassed the 0.03% per surface level. A feature of the UDRI  $\lambda/2$  data is the significant number of negative absorptions. This may be an indication of severe problems of scattering.

Northrop submitted absorption data for some of their deliverable samples and subsequently remeasured two samples. Two samples were sent to Raytheon. Tables 17 and 18 list their results. These measurements are compared in Tables 19. Samples 1146 and 1147 were measured in all three calorimeters. Northrop and Raytheon are in very good agreement. However, the UDRI data for both the bare and the AR coated substrates



1163



1078

Figure 7. Bulk Optical Uniformity of Single Crystal and Polycrystalline  $\text{CaF}_2$ , Twyman-Green

TABLE 10  
FLATNESS OF POLISHED SUBSTRATES GIVEN IN FRACTIONS OF  
A WAVELENGTH AT 5461 Å. (PEAK TO PEAK)

Sample#	Flatness		Type
	Side 1	Side 2	
1074	3/4	2	Polycrystalline
1078	3/4	1/4	Polycrystalline
1079	3 3/4	3/2	Polycrystalline
1081	1/2	1/4	Polycrystalline
1138	3/2	1/2	Single Crystal
1148	1	1	Single Crystal
1152	4	6 1/2	Single Crystal
1163	1/8	1/8	Single Crystal

TABLE 11  
 ABSORPTION DATA (UDRI) FOR COATING DESIGN 1

SAMPLE NO. XTAL CaF <sub>2</sub>	THICKNESS (cm)	MASS (gm)	A <sub>U</sub> × 10 <sup>-3</sup>	A <sub>C</sub> × 10 <sup>-3</sup>	ΔA × 10 <sup>-3</sup>
1136	1.06	67.80	1.31	2.67	1.36
1135	1.07	68.50	1.455	13.40	11.95
1134	1.07	68.48	1.92	4.07	2.15
POLY CaF <sub>2</sub>					
1084	0.930	59.42	1.42	2.88	1.46
1076	.940	55.37	1.65	2.28	0.68
POLY BaF <sub>2</sub>					
1180	.875	85.83	1.88	3.07	1.19
1173	1.00	98.27	2.26	3.61	1.35

TABLE 12  
 ABSORPTION DATA (UDRI) FOR COATING DESIGN 2

SAMPLE NO.	THICKNESS (cm)	MASS (gm)	$A_u \pm 10^{-3}$	$A_c \pm 10^{-3}$	$\Delta A \pm 10^{-3}$
XTAL $\text{CaF}_2$					
1144	1.02	65.80	1.78	2.19	0.41
1145	1.015	65.80		2.26	
1146	1.03	66.18	1.75	1.48	-0.27
1147	1.02	65.43	1.50	1.11	-0.39
1148	1.03	66.32	1.71		
POLY $\text{CaF}_2$					
1077	.960	61.61	1.67	1.27	-0.4
1089	.960	61.39	1.56	1.75	0.19
1072					
1082					
1081	.960	61.54	2.11		
POLY $\text{BaF}_2$					
1164	.995	97.53	1.20	1.53	0.33
1172	.995	97.87	1.47	1.71	0.24

TABLE 13  
 ABSORPTION DATA (UDRI) FOR COATING DESIGN 3

SAMPLE NO.	THICKNESS (cm)	MASS (gm)	$A_U \pm 10^{-3}$	$A_C \pm 10^{-3}$	$\Delta A \pm 10^{-3}$
XTAL $\text{CaF}_2$					
1151	1.065	68.08	1.32	7.69	6.37
1153	1.06	67.52	1.55	8.50	6.95
1149	1.07	68.54	2.06	6.54	4.48
1150	1.065	67.87	1.81	1.89	0.08
POLY $\text{CaF}_2$					
1086	.965	62.07	1.16	7.24	6.08
1087	.970	62.48	1.25	8.44	7.19
POLY $\text{BaF}_2$					
A	.815	79.40	1.28	5.46	4.18
1178			—	—	—

TABLE 14

ABSORPTION DATA (UDRI) FOR COATING DESIGN 4

SAMPLE NO.	THICKNESS (cm)	MASS (gm)	$A_U \times 10^{-3}$	$A_C \times 10^{-3}$	$\Delta A \times 10^{-3}$
XTAL $\text{CaF}_2$					
1162	.985	63.30	1.44	2.73	1.29
1160	.985	63.33	1.86	2.71	0.85
1161	.945	60.72	1.66	2.20	0.54
1159	.965	62.19	1.96	1.74	-0.22
POLY $\text{CaF}_2$					
1068	.945	60.40	3.31	1.66	1.65
1090	.985	63.25	1.83	2.71	0.88
1167	.945	60.68	1.91	1.63	-0.28
POLY $\text{BaF}_2$					
1166	.860	84.76	7.95	4.58	-3.37
1177	.865	85.11	1.71	2.92	1.21

TABLE 15

AVERAGE ABSORPTION RESULTS FROM UNCOATED AND DOUBLY  
COATED QUADRANTS OF AR COATED SPECIMENTS

Substrate	Design	$A_u \div 10^{-3}$	$A_c \div 10^{-3}$	$\Delta A \div 10^{-3}$
xtal $\text{CaF}_2$	1	1.31	2.67	1.36
	2	1.78	2.19	.41
	3	1.435	8.095	6.66
	4	1.65	2.72	1.07
Poly $\text{CaF}_2$	1	1.535	2.58	1.045
	2	1.56	1.75	.19
	3	1.21	7.84	6.63
	4	1.75	3.01	1.27
Poly $\text{BaF}_2$	1	2.07	3.34	1.27
	2	1.34	1.62	.28
	3	1.28	5.46	4.18
	4	1.71	2.92	1.21

TABLE 16  
COMPARISON OF COATING DESIGNS BY BEST ABSORPTION VALUE

Substrate/ Sample #	$(P_a/P_t)_{BARE}$	$(P_a/P_t)_{COATED}$	Per/ Surface	$\beta_{SUBSTRATE} (10^{-3} \text{cm}^{-1})$	Design
xtal $\text{CaF}_2$					
1136	.14%	.27%	.065%	1.24	1
1144	.18	.23	.025	1.70	2
1151	.14	.77	.315	1.24	3
#2	.20	.27	.035	1.89	4
Poly $\text{CaF}_2$					
1076	.17	.23	.03	1.75	1
1077	(.18)	.13	(.025)	1.73	2
1086	.12	.72	.30	1.20	3
#5	.19	.27	.04	1.86	4
Poly $\text{BaF}_2$					
1180	.20	.31	.055	2.15	1
1172	.16	.17	.005	1.46	2
A	.14	.55	.205	1.57	3
1166	(.85)	(.46)	(.195)	9.24	4

TABLE 17  
 ABSORPTION DATA OBTAINED ON NORTHROP CALORIMETER FOR 5.3 MICRONS

SAMPLE#	MATERIAL	THICKNESS	$A_u \div 10^{-3}$	$A_c \div 10^{-3}$	$\Delta A \div 10^{-3}$	$\beta$	%/SURFACE**
1072	2 PbF <sub>2</sub>	1.53 $\mu$	.805	.998	.194	.6cm <sup>-1</sup>	
1082	2 ThF <sub>4</sub>	1.78	1.05	1.21	.16	.4	
1089	2 AR		.89	.41	(.47)		(-)
1164	2 AR		.76	.92	.16		
1144	1 AR		.48	.51	.03		.003
1144	1 AR			.50	.02		.002
1146	2 PbF <sub>2</sub>	1.53	.49	1.02	.53	1.7	
1147	2 ThF <sub>4</sub>	1.78	.44	.98	.54	1.5	
1145*	2 AR		.44	.81	.37		.02
1144*	2 AR		.76	.89	.13		.007

\* Data obtained 10/15/75 approximately six months after other data

\*\* CaF<sub>2</sub> substrates

TABLE 18  
 ABSORPTION DATA OBTAINED ON RAYTHEON CALORIMETER FOR 5.3 MICRONS

SAMPLE#	MATERIAL	THICKNESS	$A_u \div 10^{-3}$	$A_c \div 10^{-3}$	$\Delta A \div 10^{-3}$	$\beta_f = \Delta A / +$
1146	PbF <sub>2</sub>	1.53 $\mu$	.58	1.06	.48	1.57 cm <sup>-1</sup>
1147	ThF <sub>4</sub>	1.78 $\mu$	.46	.79	.33	.93

\* Data is for the doubly coated quadrant

TABLE 19  
COMPARISON OF 5.3 MICRON CALORIMETER  
ABSORPTION MEASUREMENTS ON  $\text{CaF}_2$

## BARE SUBSTRATE

Sample	UDRI/Raytheon	Northrop/Raytheon
1146	3	.88
1147	3.2	.93

## HALF-WAVE COATED SUBSTRATES

Sample	Northrop/Raytheon
1146 ( $\text{PbF}_2$ )	.96
1147 ( $\text{ThF}_4$ )	1.2

## AR COATED SUBSTRATES

Sample	UDRI/Northrop
1144	2.7
1145	3.4

is approximately a factor of three higher. Raytheon - Northrop substrate absorptions yield betas in the  $10^{-4} \text{ cm}^{-1}$  range which at the present time is of the order of the generally accepted value. This would seem to indicate that the coating absorptions given in Tables 15 and 16 are pessimistic.

Absorption data at 1.06 was obtained by O'Brien (Reference 8) at AFIT and at 3.8 by Harrington (Reference 9) at the University of Alabama. The results are listed in Tables 20, 21, and 22. The substrate absorption at 1.06 is far above the intrinsic value (extrapolation of multiphonon exponential dependence) and it is comparable to the 5.3 micron absorption. This same result was obtained for the bulk values at 3.8 microns. At 1.06,  $\text{PbF}_2$  has a fairly high absorption coefficient ( $\sim 25 \text{ cm}^{-1}$ ). Its beta at 3.8 is approximately ten times its value at 5.3. At 1.06,  $\text{ThF}_4$  has a low absorption coefficient ( $\sim 1 \text{ cm}^{-1}$ ) and its beta at 3.8 is also approximately ten times its value at 5.3. The absorption of an AR coating at 3.8 should then be approximately seven times the value at 5.3. Using the Northrop values for AR absorption (1144) at 5.3 given in Table 17 indicates that absorptions per surface for 3.8 AR coatings can be as low as 0.01 - 0.02%.

### 3. OPTICAL SPECTRA

Infrared transmission and reflectance scans were delivered by the various vendors. Hughes Research Laboratory and Northrop Research and Development Center submitted transmission scans obtained on Beckman infrared spectrophotometers. Perkin-Elmer and Valpey submitted transmission scans obtained on a Perkin-Elmer 180 spectrophotometer. Perkin-Elmer also delivered reflectivity scans of witness wedges for every coating delivered on the 5X scale using as a calibration the single surface reflectivity (17.4%) of a ZnSe wedge. Valpey delivered reflectivity scans of antireflection-coated substrates, whose opposite side was ground, on the 10x scale using as a calibration the single surface reflectivity (2.7%) of a  $\text{CaF}_2$  wedge. An example of each is shown in Figures 8 and 9.

TABLE 20  
ABSORPTION OF  $\text{CaF}_2$  AT 1.06 MICRONS

Sample#	$\beta:10^{-4}$
1202	5.1 $\text{cm}^{-1}$
1203	10.0
1204	7.9
1205	3.4

$\beta = 6.6 \times 10^{-4} \text{cm}^{-1}$

TABLE 21  
ABSORPTION OF  $\lambda/2$  COATINGS AT 1.06 MICRONS

SAMPLE#	MATERIAL	THICKNESS	$A_u:10^{-3}$	$A_c:10^{-3}$	$\Delta A:10^{-3}$	* $\beta_f = \Delta A/+$	$\beta_f$
1146	$\text{PbF}_2$	1.53 $\mu$	.188	4.1	3.9	25 $\text{cm}^{-1}$	
1147	$\text{ThF}_4$	1.78	.123	.31	.187	1	

\* ignores interference effects

TABLE 22  
ABSORPTION OF SINGLE LAYER\* COATINGS AT 3.8 MICRONS

SAMPLE#	MATERIAL#	THICKNESS	$A_u:10^{-3}$	$A_c:10^{-3}$	$\Delta A:10^{-3}$	** $\beta = \Delta A/+$
1072	$\text{PbF}_2$	1.53	.54	1.14	.6	3.9 ( $\text{cm}^{-1}$ )
1082	$\text{ThF}_4$	1.78	1.67	2.22	.55	3.1
1070	$\text{ZrO}_2$	1.36	5.36	47.9	42.5	31.3
1073	$\text{ThF}_4$	1.78	.35	1.7	1.35	7.6
1085	$\text{PbF}_2$	1.55	1.9	2.7	.8	5.2

\* layer thickness equal to  $\lambda/2$  at 5.3 microns

\*\* ignores interference effects

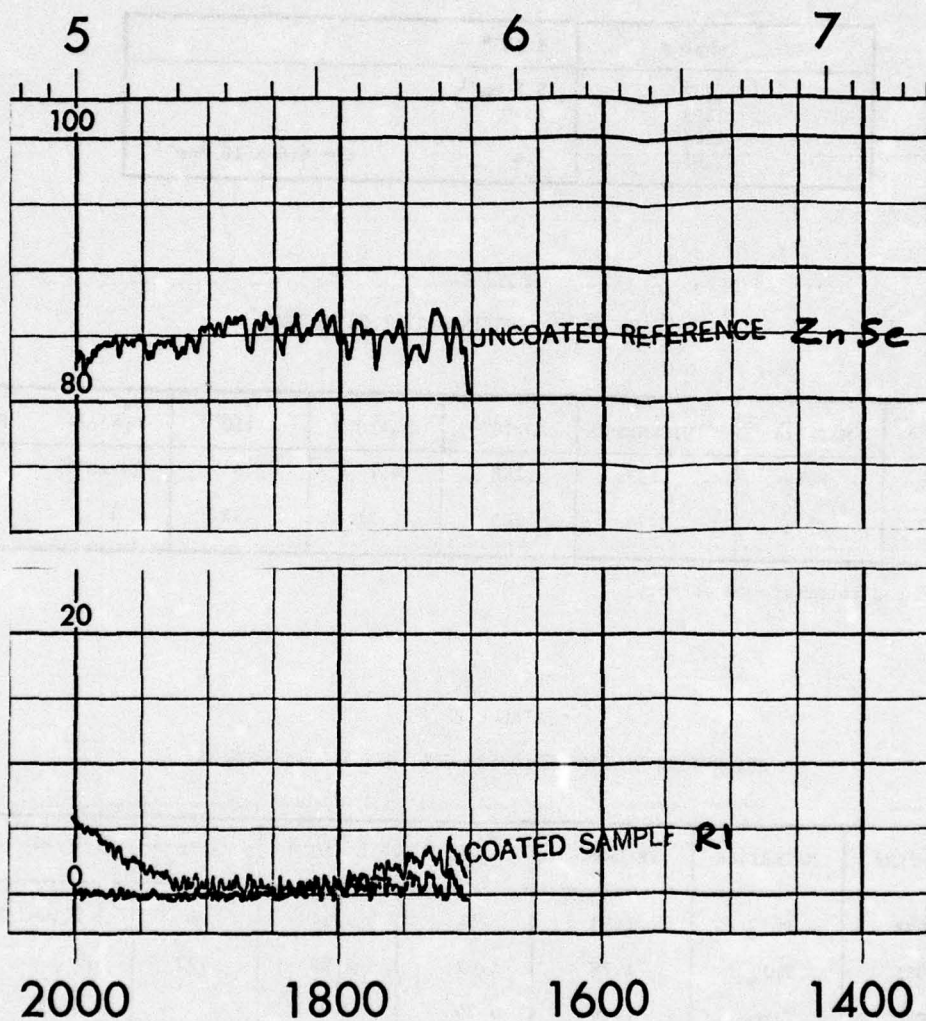


Figure 8. Single Surface Reflectance for CaF<sub>2</sub> Witness Wedge for Sample 1087 for Side R1. Data Obtained by Perkin-Elmer on P-E 180 Spectrophotometer (5X)

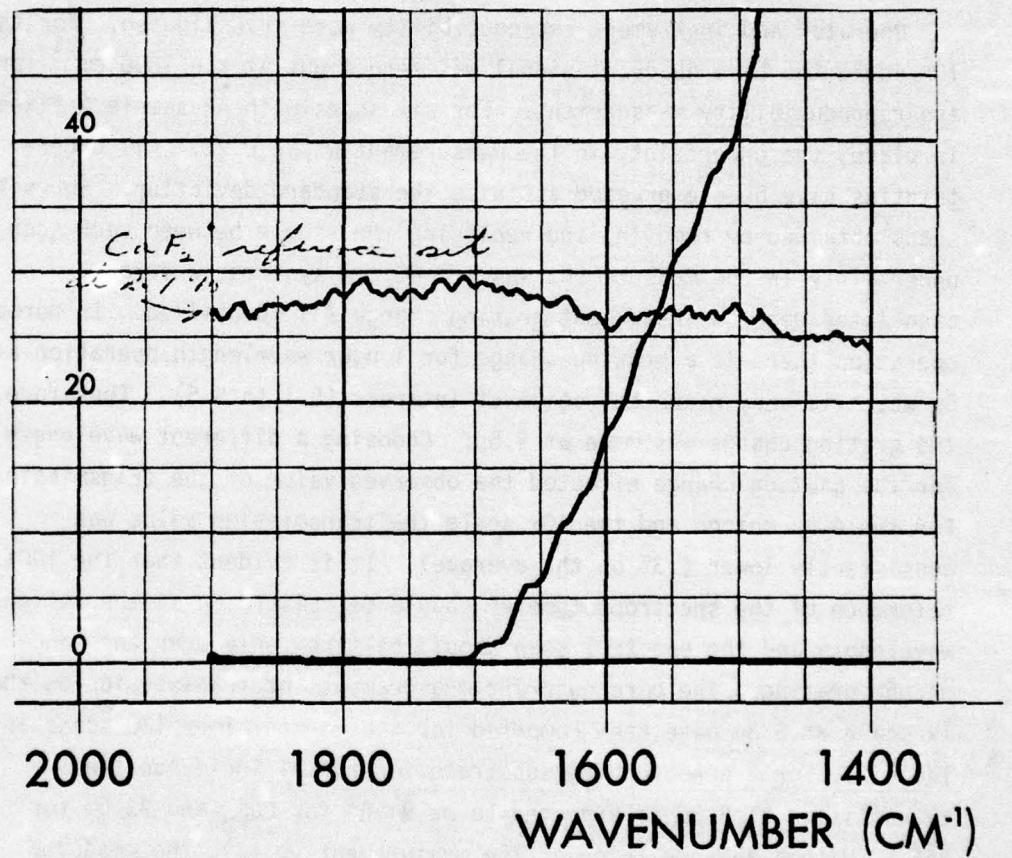


Figure 9. Single Surface Reflectance for AR Coated CaF<sub>2</sub> Witness Piece Obtained by Valpey on a P-E 180 Spectrophotometer (10X)

In order to compare the performance of the (AR) coated samples supplied by the different vendors all of the AR coated polycrystalline  $\text{CaF}_2$  and  $\text{BaF}_2$  substrates were measured on a Perkin-Elmer 180 by a single operator at the University of Miami. Since a reflectivity attachment was not available, only transmission scans were obtained.

Operator and instrument reproducibility were investigated. For the 10x scale the bare quadrant signal was zeroed out at  $k = 1800 \text{ cm}^{-1}$  for the reproducibility measurement. For six scans with AR sample A fixed in place, the uncertainty in the measurement was  $\pm 0.2\%$ . All uncertainties have been expressed as twice the standard deviation. For six scans obtained by removing and replacing the sample between each scan the uncertainty in the measurement was  $\pm 0.4\%$ . A systematic error associated with an instrument grating change was identified. In normal operation there is a grating change for longer wavelength operation at  $5\mu$  which is very near the region of interest (5.1 to 5.5). Therefore, the grating change was made at  $4.5\mu$ . Choosing a different wavelength for the grating change effected the observed value of the transmission. For the  $4.5\mu$  change and the 10x scale the transmission value was consistently lower (.3% on the average). It is evident that the 100% reference of the spectrophotometer should be calibrated at the design wavelength and the spectral scan should be taken only over the range of one grating. The bare quadrant measurements of transmission on the 1x scale at  $5.3\mu$  have been compared for the Perkin-Elmer 180 scans in Table 23. For a nonabsorbing substrate for normal incidence the transmission at  $5.3\mu$  is expected to be 94.6% for  $\text{CaF}_2$  and 93.5% for  $\text{BaF}_2$ . Within the precision of the measurement ( $\pm 1\%$ ), the measured value of substrate transmission is in good agreement with the expected value for all three instruments. The large uncertainty in the bare quadrant transmission creates difficulties when an attempt is made to measure transmission on the 10x scale by zeroing out the bare substrate transmission. The 10x transmission scans obtained by the zeroing process are only useful for determining the wavelength position of the peak transmission. It is possible to measure low level reflectances to within  $\pm 0.2\%$ . Finally, the optics of the instrument may present a problem. The image of the source is focused at the mid-plane of

TABLE 23

COMPARISON OF TRANSMISSION MEASUREMENTS ON BARE  $\text{CaF}_2$  AND  $\text{BaF}_2$  SUBSTRATES  
OBTAINED ON PERKIN-ELMER 180 SPECTROPHOTOMETERS BY  
PERKIN-ELMER, VALPEY, AND UNIVERSITY OF MIAMI

Substrate	# of Readings	Transmission @5.3 $\mu$	Index @5.3 $\mu$	Vendor
$\text{CaF}_2$	8	94.8 $\pm$ .7%	1.39 $\pm$ .08	P
$\text{CaF}_2$	9	95.0 $\pm$ 1.4	1.38 $\pm$ .16	V
$\text{CaF}_2$	8	94.4 $\pm$ 1.0	1.41 $\pm$ .10	M
$\text{BaF}_2$	4	92.5 $\pm$ 1.8	1.49 $\pm$ .16	P
$\text{BaF}_2$	2	92.5 $\pm$ .7	1.49 $\pm$ .06	V
$\text{BaF}_2$	7	91.9 $\pm$ 1.6	1.52 $\pm$ .10	M

a 12-inch sample chamber so the beam is converging at the sample surface making a true normal incidence measurement impossible. Some components of the beam are incident at up to 6 degrees. In reflectance, since measurements are made typically at 13 degrees or 15 degrees the problem is more serious because incident angles of 18 to 21 degrees can result. Fortunately, for the broadband coatings under consideration the problem is not severe although a collimated beam would be more desirable. However, minor shifts (tenths of microns) in the spectral response of the coatings with regard to the theoretical response may be due to alignment problems instead of incorrect coating indices. The AR coating performance scans are all taken in the constant energy mode which is obtained by cam motion at the slit. This results in a variable spot size at the sample surface which is not the ideal situation.

The AR coated polycrystalline samples were compared by the University of Miami on a relative basis using 1x transmission scans where the 100% calibration sequence was identical. Table 23 compares the University of Miami results to the Valpey and Perkin-Elmer for the bare quadrant. Table 24 summarizes the University of Miami transmission measurements on the polycrystalline substrates. Sample 1090 had the best transmission. Design 1 had the widest bandwidth (.7 to 1 $\mu$ ) and Design 3 the narrowest (.3 $\mu$ ). The bandwidth was arbitrarily defined as the range of wavelengths over which the transmission is within 0.05% of the peak transmission. The peak transmission was closest to the design value for Design 4 and slightly higher than design for all the others. Since the bandwidth of Design 3 is small and the experimental peak transmission falls above 5.3 microns the transmission at 5.3 is not optimized. The experimental transmission vs wavelength scans for the four designs are given in Figures 10 and 11. Generally, the transmission for the AR coated BaF<sub>2</sub> is poor. The best result was obtained on a single crystal. Table 25 combines the wedge angle reflectance data of Perkin-Elmer and the absorption data of UDRI. The calculated transmission in Table 25 assumes no scattering loss. Table 26 compares calculated transmission and observed transmission where data was available from the three Perkin-Elmer 180 spectrophotometers.

TABLE 24  
TRANSMISSION OBTAINED ON 1X SCALE OF PERKIN-ELMER 180  
SPECTROMETER BY UNIVERSITY OF MIAMI

Substrate Sample#	Vendor	Transmission ( $\pm 1\%$ )			Peak Trans	Bandwidth*	$\Delta\lambda$	Peak $\lambda(10X)$
		5.1	5.3	5.5				
Poly CaF <sub>2</sub>								
0089	1	99.2	99.4	99.3	99.4	4.70-5.70	1.00	—
0096	1	98.2	98.9	99.0	99.0	5.20-5.77	.52	—
1077	2	97.2	97.9	97.8	98.0	5.2 -5.68	.48	5.40
1089	2	98.8	99.0	99.0	99.1	5.08-5.62	.54	5.40
1086	3	97.4	98.4	98.6	98.9	5.30-5.65	.35	—
1087	3	96.1	98.0	98.4	98.5	5.35-5.70	.35	—
2	4	98.6	98.3	97.9	98.6	5.00-5.50	.50	5.30
5	4	100.0	100.0	98.8	100.0	4.85-5.60	.75	5.32
Poly BaF <sub>2</sub>	4							
1173	1	96.4	96.9	97.0	97.0	5.1 - 5.8	.70	5.55
1180	1	—	—	—	—	—	—	—
1164	2	97.0	97.2	97.0	97.2	4.90-5.70	.80	5.32
1172	2	96.4	97.0	97.2	97.2	5.10-5.90	.80	5.45
A (xtal)	3	97.5	98.3	98.6	98.6	5.20-5.60	.40	—
—	3	—	—	—	—	—	—	—
1166	4	95.2	95.2	94.9	95.2	4.90-5.60	.70	5.25
1177	4	96.1	96.4	95.9	96.4	5.00-5.60	.60	5.25

\*Wavelength region over which transmission is within .05% of peak.

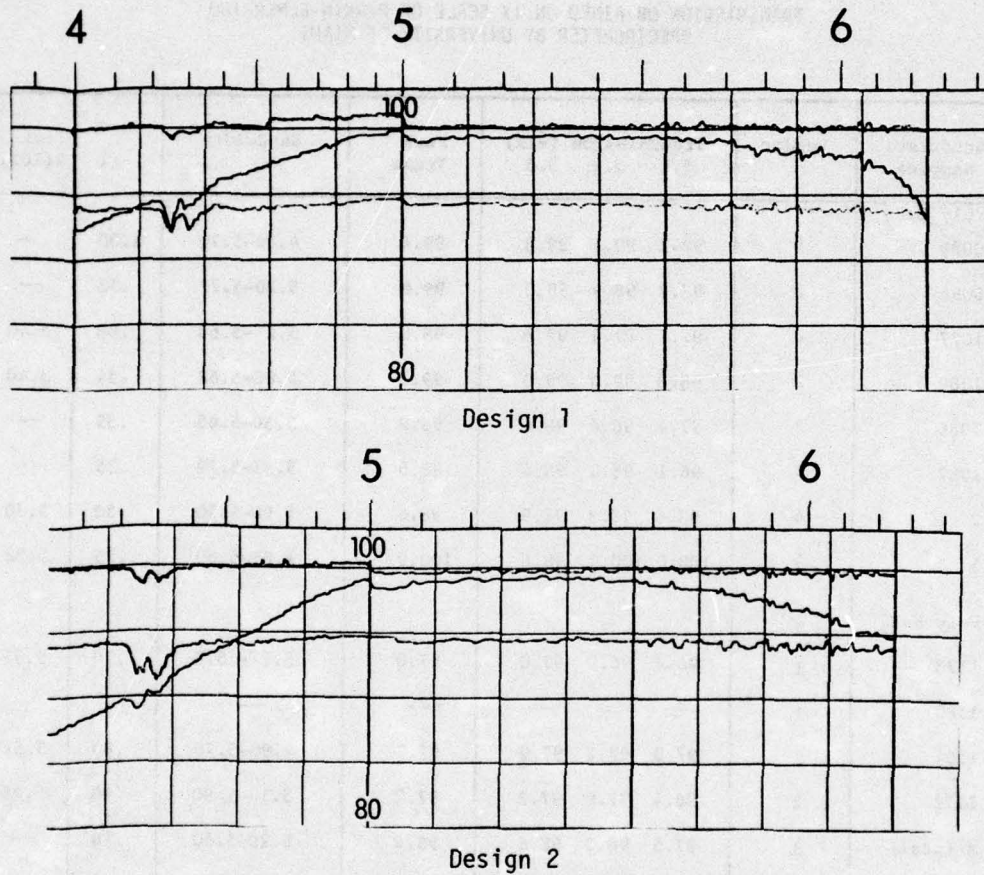
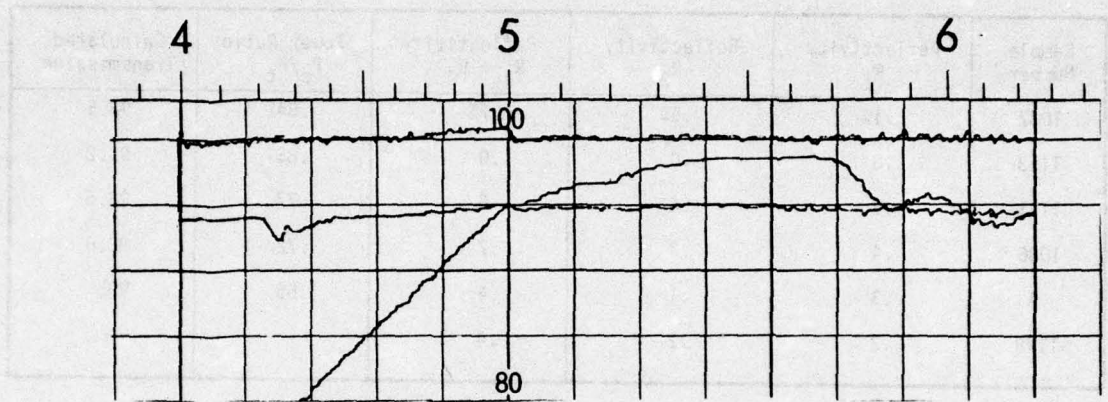
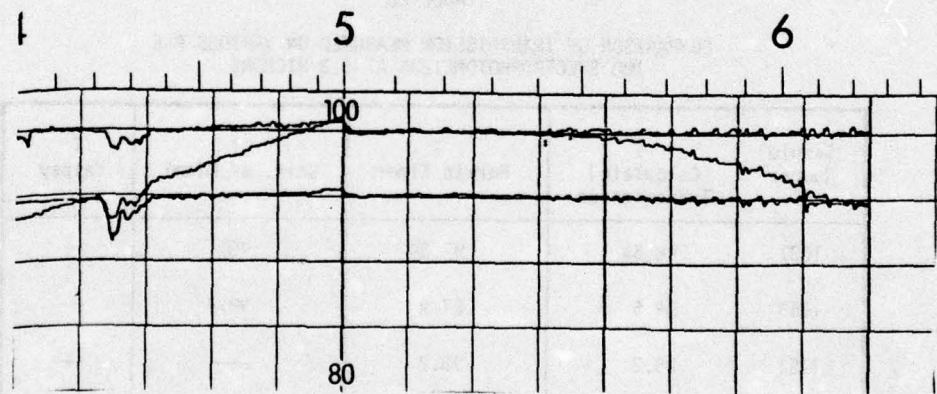


Figure 10. Experimental Transmission vs Wavelength (P-E 180) for Design 1 (10a) and Design 2 (10b) on Polycrystalline  $\text{CaF}_2$ . The Upper Trace is the 100% Calibration Line. The middle Trace is for the Quadrant AR Coated on Both Sides. The Lower Trace is the Bare Substrate



Design 3



Design 4

Figure 11. Experimental Transmission vs Wavelength (P-E 180) for Design 3 (11a) and Design 4 (11b) on Polytran CaF<sub>2</sub>. The Upper Trace is the 100% Calibration Line. The Middle Trace is for the Quadrant AR Coated on Both Sides. The Lower Trace is the Bare Substrate

TABLE 25  
SINGLE SURFACE REFLECTIVITY OF AR COATED WITNESS WEDGES  
(PERKIN-ELMER)

Sample Number	Reflectivity $R_1$	Reflectivity $R_2$	Reflectivity $R_1 + R_2$	Power Ratio $P_a/P_t$	Calculated Transmission
1087	.1%	.6%	.7%	.84%	98.5
1153	.0	.0	.0	.85	99.2
1151	.2	.4	.6	.77	98.6
1086	.4	.3	.7	.72	98.6
A	.3	.1	.4	.55	99
1178	.2	.2	.4	—	—

TABLE 26  
COMPARISON OF TRANSMISSION MEASURED ON VARIOUS P-E  
180 SPECTROPHOTOMETERS AT 5.3 MICRONS

Sample Number	T Calculated Transmission	T Perkin Elmer	T Univ. of Miami	T Valpey
1087	98.5%	97.5%	98%	—
1153	98.6	97.9	98.4	—
1151	99.2	98.2	—	—
1086	98.6	98.1	—	—
A	99.0	98.7	98.3	—
1177	—	—	96.4	96.75
1166	—	—	95.2	97.75
5	—	—	100.0	99.1
2	—	—	98.3	100.0

Reflectance spectra for the half-wave coatings were obtained by UDRI in the wavelength range between 0.5 and 2.2 $\mu$ m and the fringe analysis technique was used to determine the optical thickness. These results utilizing the film design indices were compared to the physical thickness measured on a Sloan Dectak profilometer. Table 27 lists the results. For SrF<sub>2</sub> there is a substantial disagreement. It appears that SrF<sub>2</sub> in half-wave thickness has an index lower than 1.33, approximately 1.22.

#### 4. COATING QUALITY

Visual inspection of the samples revealed that S1 of 1178 (AR coated Polytran BaF<sub>2</sub> with ZrO<sub>2</sub>/ThF<sub>4</sub>) had flaked off. Within two months of delivery S2 of sample A (AR coated single crystal BaF<sub>2</sub>) also flaked off. The SrF<sub>2</sub> half-wave coatings, S2 of 1074 (Polytran CaF<sub>2</sub>) and 1134 (SC CaF<sub>2</sub>), also flaked off after several months. Crossed-polarizer shots of the SC CaF<sub>2</sub> and the Polytran BaF<sub>2</sub> substrates were taken prior to shipment to the coating vendors. Crossed-polarizer shots of the coated substrates were taken after delivery to AFML. Figure 12 shows a before and after comparison of Hughes AR Polytran BaF<sub>2</sub> for sample 1180. The strain pattern appears to reproduce the grain structure of the substrate. This effect was observed in one Valpey  $\lambda/2$  coating (sample 1067, Polytran CaF<sub>2</sub>) and in two other Hughes Polytran samples (1173 and 1180). Samples 1160 and 1162 shown in Figure 13 have a streaky strain pattern. Half-wave coatings showing residual strain in the coating were the SrF<sub>2</sub> layer on 1134 and 1075 and layer one on 1161 and 1067 and a slight amount in layer two on 1071. In summary, the Perkin-Elmer and the Northrop coatings showed no residual strain, the Hughes SrF<sub>2</sub> and AR coatings showed severe strain on Polytran CaF<sub>2</sub> and BaF<sub>2</sub> substrates, and the Valpey layer #1 and AR coating showed severe strain on Polytran CaF<sub>2</sub> moderate strain on SC CaF<sub>2</sub> but none on Polytran BaF<sub>2</sub>. It appears that PbF<sub>2</sub>, ThF<sub>4</sub> or ZrO<sub>2</sub> can easily be deposited in a strain-free condition as a first layer on CaF<sub>2</sub> or BaF<sub>2</sub> substrates.

After all of the optical measurements were completed, the adhesion of the AR coatings was evaluated. Scotch tape tests (Table 28) were made

TABLE 27  
 COMPARISON OF OPTICAL THICKNESS AND PHYSICAL THICKNESS  
 FOR HALF-WAVE COATINGS

SAMPLE# *	SIDE	COATING MATERIAL	OPTICAL THICKNESS ( $\mu$ )	PHYSICAL THICKNESS ( $\mu$ )	AVG. DEKTAK THICKNESS ( $\mu$ )
1146	1	$\lambda/2$ PbF <sub>2</sub>	2.7	1.561	1.550
	2	$\lambda/2$ PbF <sub>2</sub>	2.69	1.555	1.550
1147	1	$\lambda/2$ ThF <sub>4</sub>	2.59	1.738	1.700
	2	$\lambda/2$ ThF <sub>4</sub>	2.56	1.718	1.650
1149	1	$\lambda/2$ ZrO <sub>2</sub>	2.69	1.380	1.367
	2	$\lambda/2$ ZrO <sub>2</sub>	2.69	1.380	1.350
1150	1	$\lambda/2$ ThF <sub>4</sub>	2.61	1.752	1.750
	2	$\lambda/2$ ThF <sub>4</sub>	2.67	1.792	1.750
1075	1	$\lambda/2$ PbF <sub>2</sub>	2.635	1.541	1.500
	2	$\lambda/2$ SrF <sub>2</sub>	2.315	1.728	1.883
1134	1	$\lambda/2$ PbF <sub>2</sub>	2.703	1.581	1.450
	2	$\lambda/2$ SrF <sub>2</sub>	2.375	1.772	1.937
1137	1	$\lambda/2$ PbF <sub>2</sub>	2.67	1.561	1.483
	2	$\lambda/2$ SrF <sub>2</sub>	2.55	1.903	1.783

\*In all cases the substrate material is CaF<sub>2</sub>

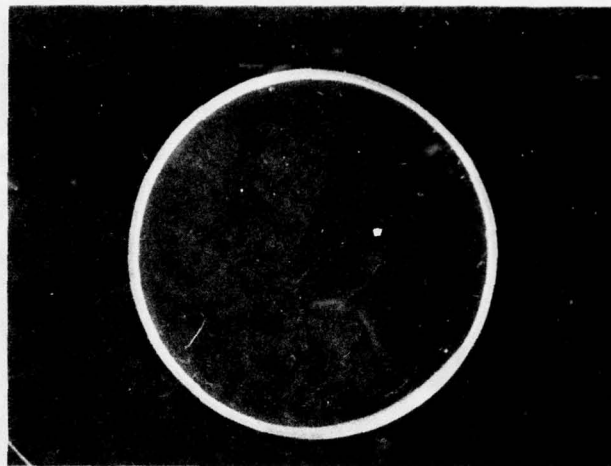


Figure 12. Strain Induced Birefringence in Visible Crossed-Polarizer Shot, Before Coating (Top), and After AR Coating (Bottom). The Quadrant Format is Visible. (Sample 1173)

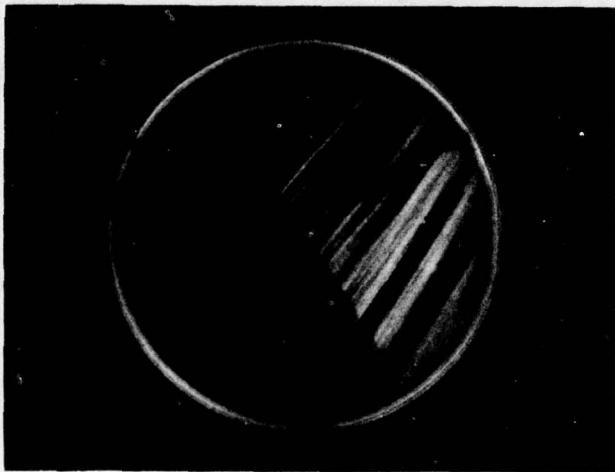
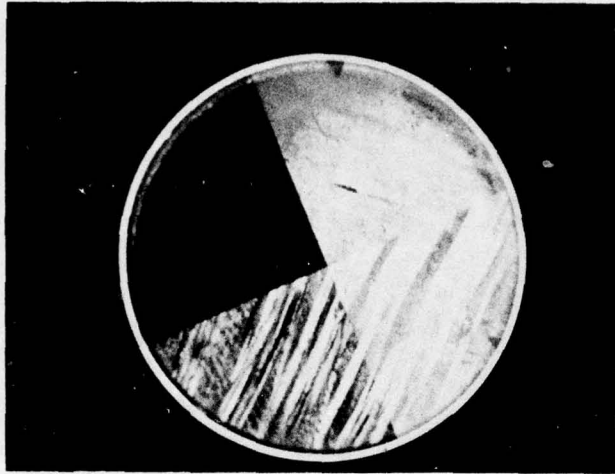


Figure 13. Sample of Streaky Residual Strain Patterns, Sample 1076 (Top) and Sample 1068 (Bottom). Crossed-Polarizer Shot

TABLE 28  
SCOTCH TAPE ADHESION TEST OF AR COATED SUBSTRATES

Sample#	Design	Pass/Fail
1144	2	P
1151	3	P
1160	4	P
1076	1	F
1087	3	P
1177	4	P
1172	2	P
1180	1	P

some six months after the samples were initially received. By that time, the  $\text{SrF}_2$  outer layer of Design 1 was cloudy, which may account for the failure of sample 1076 to pass the scotch tape test. All other samples tested, passed. Toppole test data was obtained for each design and each type of substrate. The adhesion data in arbitrary units is given in Table 29. The 260-gram force obtained for Design 1 compares favorably with the adhesion of metal films on glass.

All of the coatings were water white except for the  $\text{SrF}_2$  films which were rough and cloudy in appearance. There was so little scatter in the visible that one had to look carefully to determine the coated quadrants.

The zirconium dioxide  $\lambda/2$  coatings displayed an anomalous behavior, possibly indicating an index grading characteristic of oxygen deficiencies. Table 30 lists the single surface reflectances obtained by Perkin-Elmer

TABLE 29  
TOPPLE TEST ADHESION DATA (UDRI)

DESIGN	SUBSTRATE		VENDOR AVERAGE (Polycrystalline Data Only)
	Single CaF <sub>2</sub>	Polycrystalline BaF <sub>2</sub> CaF <sub>2</sub>	
1	---- <sup>a</sup> ----	234.2 <sup>c</sup> 265.0 <u>231.4</u> <u>315.9</u>	261.6
2	110.7 <u>129.8</u>	99.5    158.6 <u>56.5</u> <u>68.7</u>	95.8
3	89.4 <u>37.7</u>	91.6    100.2 ---- <sup>b</sup> <u>40.7</u>	60.2
2	---- <sup>a</sup> <u>26.4</u>	34.0    75.3 <u>57.0</u> <u>40.4</u>	51.7

Substrate  
Average            78.8            114.9            133.1

- a No samples available
- b Sample crazed
- c Arbitrary units

TABLE 30  
 HALF-WAVE COATING SINGLE SURFACE REFLECTANCE  
 FROM PERKIN-ELMER DATA

Sample Number	Side	Reflectance $\Delta R^*$		Material
1070	R1	2.1%	-0.6%	ZrO <sub>2</sub>
1070	R2	4.6	+1.9	ZrO <sub>2</sub>
1149	R1	2.4	-0.3	ZrO <sub>2</sub>
1149	R2	4.1	+1.4	ZrO <sub>2</sub>
1073	R1	3.2	+0.5	ThF <sub>4</sub>
1073	R2	3.1	+0.4	ThF <sub>4</sub>
1150	R1	3.0	0.3	ThF <sub>4</sub>
1150	R2	3.2	+0.5	ThF <sub>4</sub>

on their half-wave coatings at the design wavelength. The expected reflectance is 2.7% and the ThF<sub>4</sub> coatings had a reflectance of 3.1% for S1 and S2. From a comparison of the optical thickness obtained from interference fringe analysis and the physical thickness as measured on a Dek-tak shown in Table 27, it appears that the discrepancy between the measured and theoretical reflectance is attributable to the limitation of photometric accuracy. For 20 determinations of the single surface reflectance of ZnSe the results were  $17.2\% \pm 0.4$  as compared to the theoretical value of 17.4%. Therefore, the accuracy of the reflectance measurement is  $\pm 0.4 - 0.5\%$ . Table 30 indicates that for the ZrO<sub>2</sub>  $\lambda/2$  coatings S1 has a significantly different reflectance from S2. S1 was deposited simultaneously on 1070 and 1149 and similarly S2 was deposited simultaneously on 1070 and 1149. S1 appears to be behaving normally but the reflectance of side S2 is high. Transmission scans for 1070 are shown in Figures 12 and 13. In Figure 14, the transmission of S1 is nearly equal to that of the bare substrate as it should be. However, the transmission through the quadrant coated on both sides is approximately 3% lower than that of the bare quadrant. In Figure 15 the roles of S1 and S2 are reversed. The transmission of S2 only is 3% below that of the bare quadrant. The difference in transmission cannot be attributed to absorption (see entries for S1 and S2 in Table 13). The spectral scan indicates that the coating on S2

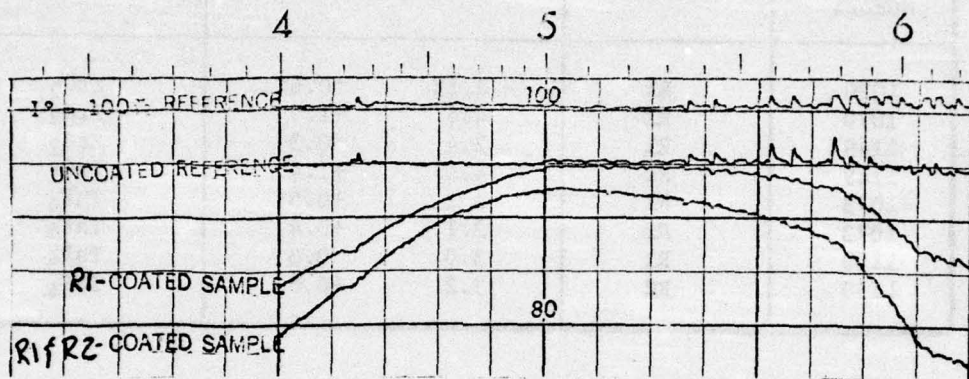


Figure 14. Transmission Scans for  $ZrO_2$  Half-wave Coating (1070).  
Beam Incident on Side R1

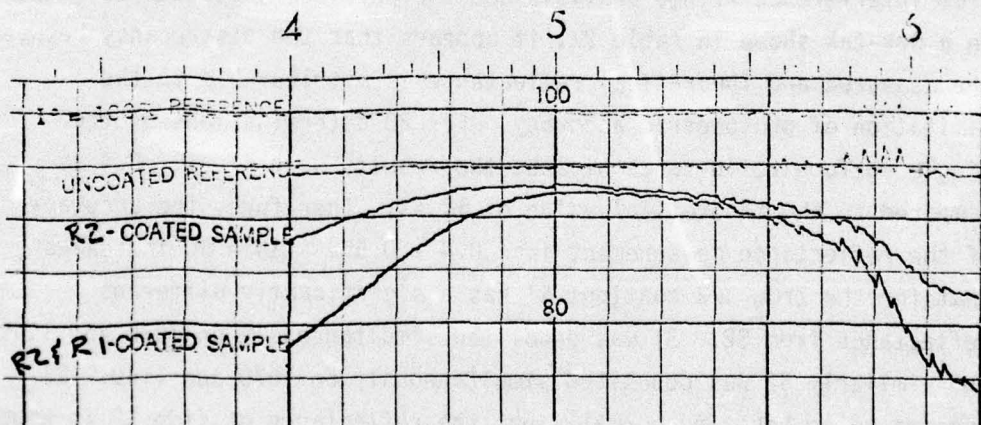


Figure 15. Transmission Scans for  $ZrO_2$  Half-wave Coating (1070).  
Beam Incident on Side R2

is peaked at the same wavelength as S1. Interference fringes from 0.5 to  $2\mu$  also coincided indicating that the optical path is identical for S1 and S2. However, the spectral scan of R2 indicates that it is not behaving as a simple one layer coating. In the visible,  $ZrO_2$  (Reference 10) has been known to have an index gradient. For glass ( $n = 1.52$ ) the reflectivity at  $\lambda/2$  is 1.25% less than uncoated which may be simulated by a double-quarter coating with indices 2.1/2.04. Oxides of titanium (Reference 11) have been used to produce index graded AR coatings for solar cells by controlling oxygen deficiencies. Titanium pentoxide has a higher index when oxygen deficient. While oxides may be hard transparent coatings at 5.3 microns it appears that stoichiometry control introduces a complexity during their deposition.

## SECTION IV

## CONCLUSIONS AND RECOMMENDATIONS

Polycrystalline  $\text{CaF}_2$  substrates are optically superior to polycrystalline  $\text{BaF}_2$ . Single crystal  $\text{CaF}_2$  is optically superior to polycrystalline  $\text{CaF}_2$ . There was little difference between the absorptions of the bare substrates polished by the four vendors. The  $\text{PbF}_2/\text{ThF}_4$  quarter-quarter AR design had the lowest absorption, below 0.04% per surface. However, the Valpey design which is reported to be capable of passing the MIL-SPEC abrasion and humidity test also had an acceptable level of absorption. It appears that the absorption of  $\text{CaF}_2$  windows at 5.3 is limited by the intrinsic absorption of  $\text{CaF}_2$ . The absorption of the design incorporating  $\text{ZrO}_2$  was excessive. The coating design incorporating  $\text{SrF}_2$  had a rough appearance and became cloudy over a period of time and on several substrates the coating failed. For all coating materials the film index was equal to the bulk index except for  $\text{SrF}_2$ . It appears that AR designs incorporating films of  $\text{CaF}_2$ ,  $\text{BaF}_2$ , and  $\text{SrF}_2$  should not be considered. Two-layer designs appear to have adequate bandwidth. However, the absorption of coating materials at 5.3 microns is so fortuitously low that more complex broadband designs with low absorption could be fabricated. All AR designs passed the scotch-tape adhesion test. Some designs were plagued with stress induced birefringence in the visible, possibly due to preferential growth rates and orientations on the large grains. However, this birefringence did not cause any problems in the IR.

Concurrent with this study, the behavior of  $\text{PbF}_2$ ,  $\text{ThF}_4$ ,  $\text{MgF}_2$ ,  $\text{BaF}_2$ , and  $\text{SrF}_2$  on oriented single crystals was investigated by Holmes and Kraatz. Samples from this program were delivered to AFML. Table 31 lists the absorption for their  $\text{PbF}_2/\text{ThF}_4$  AR design for 5.3, 3.8, and 2.8 microns. The trend is as expected. The windows at 3.8 perform as well as 10.6 windows. However, the single film data in this report and of others indicates that further work is warranted on reducing the absorption of coating materials at 2.8 and 3.8 to the level of  $0.5 - 1 \text{ cm}^{-1}$ .

TABLE 31

TOTAL ABSORPTION FOR ORIENTED SINGLE CRYSTAL  $\text{CaF}_2$   
SUBSTRATES COATED ON BOTH SIDES WITH  $\text{PbF}_2/\text{ThF}_4$ <sup>2</sup>  
QUARTER-QUARTER AR COATING

Wavelength Orientation	5.3 $\mu$ *	3.8 $\mu$	2.8 $\mu$
100	.04%	.19%	.52%
110	.03	.22	.53
111	.04	.23	.57

\* Table 35 of AFML-TR-75-188 has uncoated substrate absorption values

The characterization capability at 3.8 and 5.3 microns is not well developed. Facilities to measure low level reflectances and scattering at these wavelengths is required. The accuracy of calorimetry at 5.3 microns has not yet been established. While Raytheon and Northrop results are in agreement, they use identical calorimeters. After substantial effort the UDRI calorimeter gives absorptance values which are at least .0005 higher than the other calorimeters.

In summary, AR coatings for 5.3 microns require no further development from the standpoint of lowering the absorption. The damage threshold of the  $\text{PbF}_2/\text{ThF}_4$  and the Valpey proprietary design should be investigated at 5.3 microns. The emphasis of coating programs for the 2-6 micron region should concentrate on reducing absorption to the level of  $1 \text{ cm}^{-1}$  for HF and DF laser wavelengths. This may require a coating materials purification program. For fluoride windows, the most serious materials limitation appears to be the physical integrity of large windows.

## APPENDIX

ANALYTICAL EXPRESSIONS FOR THE INDEX AND OPTICAL THICKNESS  
OF THREE-LAYER HERPIN FILM STACKS AND OTHER  
USEFUL AR DESIGN FORMULAS

In many instances, a transparent coating material of appropriate refractive index required for a specific coating design does not exist. Fortunately, techniques have been developed for constructing equivalent films from multilayers of existing materials. The Herpin equivalent film technique has been used extensively in the development of anti-reflection coatings for ZnSe and KCl at 10.6 microns by Kurdock et al. This technique along with the results of the uniform transmission line analog technique for broadband coatings will be described in detail in this appendix. In particular, analytical expressions for the optical thickness required for each component in a three-layer Herpin equivalent for an arbitrary equivalent index and phase thickness are presented. These expressions are not included in standard references for anti-reflection coating design.

The papers of Epstein and Berning taken together provide adequate mathematical basis for Herpin film design. For the case of normally incident electromagnetic radiation the matrix method introduced by Herpin relates the fields E and H at one boundary of a film to the fields E' and H' at the other by the equation

$$\begin{pmatrix} E \\ H \end{pmatrix} = \begin{pmatrix} M_{11} & M_{12} \\ M_{21} & M_{22} \end{pmatrix} \begin{pmatrix} E' \\ H' \end{pmatrix} \quad (1)$$

The matrix for a homogeneous film of index n and physical thickness is

$$\begin{pmatrix} \cos(2\pi n x / \lambda_0) & (i/n) \sin(2\pi n x / \lambda_0) \\ i n \sin(2\pi n x / \lambda_0) & \cos(2\pi n x / \lambda_0) \end{pmatrix} \quad (2)$$

where  $\lambda_0$  is the wavelength in free space and the optical phase thickness of the film is  $\phi (\phi = 2\pi n x / \lambda_0)$ .

The determinant of the matrix(M) is unity and for nonabsorbing media  $M_{11}$  and  $M_{22}$  are real and  $M_{12}$  and  $M_{21}$  are totally imaginary. If several films or film combinations are combined the matrix for the whole is obtained from the matrices of the parts by multiplying the latter together in order in the direction of incidence.

$$M_s = M_1 * M_2 * M_3 - - - M_i \quad (3)$$

If two different film systems are described by the same matrix they are defined to be equivalent. The matrix of a single film always has  $M_{11}=M_{22}$ . Herpin's theorem states that any thin film combination is equivalent, in general, at one wavelength to a two-film combination, but not necessarily to a single film. In the particular case where the thin film combination is symmetric the equivalent film is a single film regardless of wavelength. This latter statement is true because the diagonal elements of the matrix for the symmetric stack are equal and the components of the matrix may always be set equal to

$$\begin{aligned} M_{11}=M_{22} &= \cos \mu \\ N &= (i \sin \mu) / M_{12} = -i M_{21} / \sin \mu, \end{aligned} \quad (4)$$

where N is the equivalent index and  $\mu$  is the equivalent phase thickness.

Consider symmetric three-layer film combinations of the form pqp where the p layers have equal thickness and index. Let their values be respectively  $\phi_p$  and  $n_p$  and for the q layer let the corresponding values be  $\phi_q$  and  $n_q$ . The matrix of this three-layer combination obtained by multiplying the individual matrices together in order is:

$$\begin{aligned} M_{11}=M_{22} &= \cos 2\phi_p \cos \phi_q \\ &- 1/2(n_q/n_p + n_p/n_q) \sin 2\phi_p \sin \phi_q, \end{aligned} \quad (5)$$

$$\begin{aligned} M_{12} &= (i/n_p) \{ \sin 2\phi_p \cos \phi_q \\ &+ 1/2(n_p/n_q + n_q/n_p) \cos 2\phi_p \sin \phi_q \\ &+ 1/2(n_p/n_q - n_q/n_p) \sin \phi_q \}, \end{aligned} \quad (6)$$

$$M_{21} = i n_p \left\{ \sin 2\phi_p \cos \phi_q + \frac{1}{2} \left( \frac{n_p}{n_q} + \frac{n_q}{n_p} \right) \cos 2\phi_p \sin \phi_q - \frac{1}{2} \left( \frac{n_p}{n_q} - \frac{n_q}{n_p} \right) \sin \phi_q \right\}. \quad (7)$$

Changing notation slightly such that  $n_p = n_1$ ,  $\phi_p = \phi_1$ ,  $n_q = n_2$ ,  $\phi_q = \phi_2$ , and that  $q = 2\phi_1/\phi_2$ ,  $\sigma = 2\phi_1 + \phi_2 =$  phase thickness of the three-film system allows Equations 5 to 7 to be rewritten as

$$N^2 = n_1^2 \left\{ \frac{\sin \frac{q\sigma}{1+q} \cos \frac{\sigma}{1+q} + \frac{1}{2} \left( \frac{n_1}{n_2} + \frac{n_2}{n_1} \right) \cos \frac{q\sigma}{1+q} \sin \frac{\sigma}{1+q} - \frac{1}{2} \left( \frac{n_1}{n_2} - \frac{n_2}{n_1} \right) \sin \frac{\sigma}{1+q}}{\sin \frac{q\sigma}{1+q} \cos \frac{\sigma}{1+q} + \frac{1}{2} \left( \frac{n_1}{n_2} + \frac{n_2}{n_1} \right) \cos \frac{q\sigma}{1+q} \sin \frac{\sigma}{1+q} + \frac{1}{2} \left( \frac{n_1}{n_2} - \frac{n_2}{n_1} \right) \sin \frac{\sigma}{1+q}} \right\} \quad (8)$$

$$\cos \gamma = \cos \frac{q\sigma}{1+q} \cos \frac{\sigma}{1+q} - \frac{1}{2} \left( \frac{n_1}{n_2} + \frac{n_2}{n_1} \right) \sin \frac{q\sigma}{1+q} \sin \frac{\sigma}{1+q}, \quad (9)$$

$$\sin^2 \gamma = \left[ \sin \frac{q\sigma}{1+q} \cos \frac{\sigma}{1+q} + \frac{1}{2} \left( \frac{n_1}{n_2} + \frac{n_2}{n_1} \right) \cos \frac{q\sigma}{1+q} \sin \frac{\sigma}{1+q} \right]^2 - \frac{1}{4} \left[ \left( \frac{n_1}{n_2} - \frac{n_2}{n_1} \right) \sin \frac{\sigma}{1+q} \right]^2. \quad (10)$$

The consequences of Equations 8 - 10 have been investigated thoroughly by Epstein and Berning for various values of the ratio  $q$ . For period thicknesses such that  $\sin x \approx x$  and  $\cos x \approx 1$ ,  $N$  and  $\mu$  are given by

$$N \approx n_1 \left( \frac{q + n_2/n_1}{q + n_1/n_2} \right)^{1/2}, \quad (11)$$

$$\mu \approx \sigma \left( 1 + \frac{(n_1 - n_2)^2 q}{n_1 n_2 (1+q)^2} \right)^{1/2} \quad (12)$$

Equation 12 indicates that  $\mu$  is linearly related to  $\sigma$  and investigation of the exact equations for  $\mu$  indicate that for known materials Equation 12 remains valid to values exceeding 90 degrees. However the range of Equation 11 is quite restricted. Usually one is interested in obtaining the physical thicknesses  $\phi_1$  and  $\phi_2$  which will yield the required  $N$  and  $\mu$ . It is possible to obtain analytical expression for  $\phi_1$  and  $\phi_2$  in the following manner. From Equation 4

$$\frac{n_p M_{12}}{i} - \frac{M_{21}}{i n_p} = \sin \mu \left\{ n_p / N - N / n_p \right\} . \quad (13)$$

Substituting for  $M_{12}$  and  $M_{21}$  from Equations 6 and 7 and solving for  $\sin \phi_q$  yields

$$\sin \phi_q = \frac{\left( n_p / N - N / n_p \right)}{n_p / n_q - n_q / n_p} \sin \mu \quad (14)$$

Since  $\mu$  is defined in terms of its cosine, the sign of  $\sin \mu$  is undefined. This sign is conventionally chosen so that all real values of  $N$  are positive. With this additional requirement  $\mu$  is still arbitrary to within modulus  $\partial \pi$ . Equation 5 is of the form

$$a \sin 2\phi_p + b \cos 2\phi_p = c \quad (15)$$

which has the solution

$$\sin (2\phi_p + \alpha) = \frac{c}{r}, \quad \text{for } a=r\cos\alpha \\ b=r\sin\alpha \quad (16)$$

where

$$a = -\frac{1}{2} (n_q / n_p + n_p / n_q) \sin \phi_q \\ b = \cos \phi_q, \quad c = \cos \mu, \quad \tan \alpha = b/a.$$

Since a single layer antireflection coating for a substrate of index  $n_s$  is a quarter-wave optical thickness of index  $\sqrt{n_s}$  and a double quarter antireflection coating exists for which  $n_1 = \sqrt{n_s} n_2$  the expression

for quarter wave, Herpin equivalents are used extensively in coating design. For the quarter-wave situation where  $\cos \mu$  is zero, Equation 15 simplifies to

$$\text{ctn } 2\phi_p = \frac{1}{2} (n_q/n_p + n_p/n_q) \tan \phi_q \quad (17)$$

and  $\sin \mu$  in Equation 14 becomes  $\pm 1$ . For any index between  $n_p$  and  $n_q$  the three-layer equivalent coating may be HLH (High index, low index, High index) or LHL. There are two solutions corresponding to  $\sin \mu = \pm 1$ . It is possible to construct a pqp coating with a higher index than that of the high index material if it is in the order HLH and with a lower index than that of the low index material if it is in the order LHL. However, these coatings are thick, 270-degree coatings. Equation 14 yields an expression for N

$$N = \frac{-(n_p^2 - n_q^2) \sin \phi_q}{2n_q \sin \mu} \pm \frac{1}{2} \sqrt{\frac{(n_p^2 - n_q^2)^2 \sin^2 \phi_q}{n_q^2 \sin^2 \mu} + 4n_p^2} \quad (18)$$

Equation 18 can be utilized to determine the upper and lower limit for a real index constructed from two materials. For materials of respective index 1.5 and 2.42 the limits are  $.93 \leq N \leq 3.9$  and for 1.4 and 4 the limits are  $1.03 < N < 11.4$  for  $\sin \mu = \pm 1$  and  $\sin \phi_q = 1$ . The index and phase thickness of a stack of S identical symmetrical periods which are characterized by a phase thickness  $\phi$  and index N is respectively  $S\phi$  and N. This fact may be used to make non-dispersive equivalent films or film stacks with very thin layers which may be desirable from a structural point of view. For an equivalent film to be non-dispersive, the thickness of the individual layers must be small compared to the wavelength. This can always be achieved by using multiple layers of Herpin equivalents. Berning gives an example of a non-dispersive coating for a germanium substrate for the range of 3 to 10 microns which is quite practical.

The equations for Herpin equivalent coatings will be demonstrated by several examples. An antireflection coating design for ZnSe comprised of  $\text{ThF}_4$  ( $n=1.35$ ) as the inner layer and ZnSe ( $n=2.42$ ) as the outer layer

AFML-TR-76-103

can be calculated by the Herpin technique and compared to the standard two-layer design. For  $n_p$  equal to ZnSe-ThF<sub>4</sub>-ZnSe,  $n_p$  equals 2.42 and  $n_q$  equals 1.35. For the special case of one coating material identical to the substrate, a portion of the substrate acts as a coating resulting in a two-layer coating. The equivalent index required is 1.556 (equals  $\sqrt{2.42}$ ) and the equivalent phase is 90 degrees.

From Equation 14

$$\phi_q = \pm 47.63^\circ \quad \sin \phi_q = \pm \frac{(n_p/N - N/n_p)}{n_p/n_q - n_q/n_p} = \pm .7388$$

From Equation 17

$$\text{ctn } 2\phi_p = \frac{1}{2} (n_q/n_p + n_p/n_q) \quad \tan \phi_q = \pm 1.288$$

$$\phi_p = \pm 18.91^\circ$$

Solution for  $\sin \mu = +1$  ;  $2\phi_p + \phi_q = 85.45^\circ$

and

$$\frac{h_q d_q}{\lambda_0} = \frac{\phi_q}{2\pi} = .132 ; \quad \frac{h_p d_p}{\lambda_0} = \frac{\phi_p}{2\pi} = .053$$

Solution for  $\sin \mu = -1$  ;  $2\phi_p + \phi_q + 3\pi = 454.55^\circ \sim 94.55^\circ$

$$\frac{h_q d_q}{\lambda_0} = \frac{\phi_q + \pi}{2\pi} = .368 ; \quad \frac{h_p d_p}{\lambda} = \frac{\phi_p + \pi}{2\pi} = .447$$

These two solutions are identical to those given in Reference 2 that were obtained from the standard two-layer design equation (Equation 19 and 20) For Herpin indices between  $n_p$  and  $n_q$  the equivalent coatings are 90-degree coatings.

As an example of an equivalent index lower than that of either coating material consider CaF<sub>2</sub> ( $n=1.39$ ) as the outer layer and ZnSe ( $n=2.42$ ) as the inner layer on a CaF<sub>2</sub> substrate. For an antireflection coating

design pqp equal to  $\text{CaF}_2\text{-ZnSe-CaF}_2$  and  $N=1.179$  the optical thicknesses are calculated in the following fashion from Equations 14 and 17. For an index out of the range of the indices the correct solution is obtained by adding  $\pi/2$  to the value of  $\phi_p$  which results in a thick 270-degree coating. For  $\sin\mu=-1$

$$\phi_q = 16.47^\circ \qquad \phi_p = 35.55^\circ$$

$$\frac{n_q d_q}{\lambda_o} = \frac{\phi_q}{2\pi} = .046 ; \quad \frac{n_p d_p}{\lambda_o} = \frac{\phi_p + \pi/2}{2\pi} = .349$$

$$2\phi_p + \pi + \phi_q = 267.57^\circ$$

For  $\sin\mu = +1$

$$\phi_q = -16.47^\circ \qquad \phi_p = -35.55^\circ$$

$$\frac{n_q d_q}{\lambda_o} = \frac{\pi + \phi_q}{2\pi} = .454 \qquad \frac{n_p d_p}{\lambda_o} = \frac{\phi_p + \pi/2}{2\pi} = .151$$

$$2\phi_p + 2\pi + \phi_q = 272.43^\circ$$

Because the equivalent film stack for an index outside the range of the indices of the component films is a thick 270-degree coating it is standard practice to go to a double-quarter design ( $n_1 = \sqrt{n_s} n_2$ ) where it is possible to pick  $n_1$  and  $n_2$  between  $n_p$  and  $n_q$  when  $\sqrt{n_s}$  is  $< n_p$  and  $n_q$ . Then two equivalent quarter-wave stacks  $n_1$  and  $n_2$  which are 90-degree Herpin equivalents will still be thinner than a single quarter Herpin of index  $\sqrt{n_s}$ . This approach was followed by Kurdock et al. for KCl substrates with an bulk index of 1.45 which is approximately equal to the indices of  $\text{CaF}_2$ ,  $\text{SrF}_2$ , and  $\text{BaF}_2$  so the same design approach may be applied to the fluorides. As a matter of fact, the two-layer designs for KCl at 10.6 described by Loomis are approximately valid for the fluorides at the shorter wavelengths since the designs have been given in terms of optical pathlength.

Most standard references give two-layer antireflection design equations relating the squares of the tangents of both optical thicknesses to the indices  $n_1$ ,  $n_2$ , and  $n_s$ . This leads to an ambiguity in sign. The following equations involve only principle values of the tangent and give the correct signs. Optical thicknesses for negative angles are obtained by adding multiples of  $\pi$  to them.

$$\tan^2 \theta_1 = \frac{n_1^2 (n_o - n_m) (n_m n_o - n_2^2)}{(n_1^2 n_m - n_o n_2^2) (n_o n_m - n_1^2)} \quad (19)$$

$$\tan \theta_2 = \frac{n_2 (n_1^2 - n_o n_m) \tan \theta_1}{n_1 (n_o n_m - n_2^2)} \quad (20)$$

where

$n_o$  = index of refraction of substrate

$n_1$  = index of refraction of inner or bottom layer

$n_2$  = index of refraction of outer or top layer

$n_m$  = index of refraction of incident medium

$$\theta_1 = \frac{2\pi n_1 t_1}{\lambda}$$

$$\theta_2 = \frac{2\pi n_2 t_2}{\lambda}$$

Only pairs of indices lying within the shaded region of a Schuster diagram (Figure 1) can be used in Equations 19 and 20.

The output of high power lasers is distributed over a number of lines which requires AR coatings to have bandwidths of 0.3 to 0.5 microns in some instances. Muchmore has derived the requirements for an optimum bandwidth two-layer coating utilizing the uniform transmission line analogy (films have equal optical thickness). The reflection vs. wavelength for this coating shows a maximum at the design wavelength

and minimum to either side (W coating). By selecting the acceptable reflectivity at the design wavelength the indices required can be calculated from

$$n_1 = n_s^{3/4} \left[ \frac{(1-R_o)/(1+R_o)}{(1+R_o)/(1-R_o)} \right]^{1/4} \quad (21)$$

$$n_2 = n_s^{1/4} \left[ \frac{(1+R_o)/(1-R_o)}{(1-R_o)/(1+R_o)} \right]^{1/4} \quad (22)$$

and the required optical thickness ( $\psi$ ) from

$$\tan 2\psi = \frac{n_1 n_2^2 - 1}{n_2^2 - n_1/n_2} \quad (23)$$

If the indices required by Equations 21 and 22 are not available, Herpin equivalents of the correct optical thickness may be used instead to produce the optimum broadband coating.

The foregoing discussion does not represent an exhaustive treatment of AR coating design. There are many approaches to coating design and for additional information consult the list of references.

REFERENCES

1. L. Ivan Epstein, Design of Optical Filters, J. Opt. Soc. America, 42, 806 (1952).
2. Morris Braunstein and J. Earl Rudisill, Protective-Antireflective Thin Films for Polycrystalline Zinc Selenide and Alkali Halide Laser Windows, AFML-TR-75-18.
3. John R. Kurdock, Optical Processing of Alkali Halides and Polycrystalline Zinc Selenide for High-Power Laser Applications, AFML-TR-74-166, Parts I and Part II.
4. M. Braunstein, D. Zuccaro, J. Rudisill, and A. Braunstein, Low Absorption Antireflection Coatings for KCl, page 135, Proceedings of Fifth Conference on IR Laser Window Materials.
5. M. L. Bhaumik, Carbon Monoxide Laser Studies Final Report: Part I, ARPA Order No. 306, Contract No. N00014-71-C-0037.
6. H. Winston, R. Pastor, R. Turk, A. I. Braunstein, and R. F. Scholl, Fluoride Window Materials for Use as Laser Windows in the 2 to 6  $\mu$ m Spectral Region; AFML-TR-75-73.
7. Charles Strecker, Private Communication.
8. David O'Brien, Private Communication.
9. J. Harrington, Private Communication.
10. Edward Strouse, Private Communication.
11. A. Braunstein, Private Communication.

BIBLIOGRAPHY

Berning, Peter H., "Theory and Calculations of Optical Thin Films," *Physics of Thin Films*, 1, 69-121 (1963).

Berning, Peter H., "Use of Equivalent Films in the Design of Infrared Multilayer Antireflection Coatings," 52, 431 (1962).

Braunstein, A., M. Braunstein, J. Rudisill, J. Harrington, and D. Gregory, "Coating Materials for Chemical Laser Windows," p. 347, *Proc. 1975 LWC*.

Braunstein, M., Low Absorption Coating Technology, AFWL-TR-74-10.

Braunstein, M., et al., Multilayer Enhanced Dielectric Mirrors, AFWL-TR-75-196.

Braunstein, M., S. D. Allen, A. J. Braunstein, C. R. Guiliano, R. R. Turk, V. Warig, D. Zuccaro, Laser Window Surface Finishing and Coating Science, AFCRL-TR-75-0429.

Cox, J. Thomas and George Hass, "Antireflection Coatings for Optical and Infrared Optical Materials," *Physics of Thin Films*, 2, 239-304 (1964).

Dickinson, Stanley K., Property Data for ZnSe, KCl, NaCl, CaF<sub>2</sub>, SrF<sub>2</sub>, and BaF<sub>2</sub>, Technical Memo No. LQ-74-24.

Greason, P., G. Johnston, and M. Ohmer, "Comparison of the 5.3  $\mu\text{m}$  Absorption in Various AR Coatings," p. 347, *Proc. 1975 LWC*.

Harrington, James A., Low Loss Window Materials for Chemical Lasers, Semi-Annual Technical Report, July 1975, ARPA 2614, Contract # DAAH01-74-C-0437.

Holmes, S., P. Kraatz, and A. Klugman, CaF<sub>2</sub> Laser Window Study Final Report, NRTC 74-57R (1974).

Kraatz, P., S. Holmes, and A. Klugman, "Absorptance of Coated Alkaline Earth Fluoride Windows at CO Laser Wavelength," p. 315, *Proc. 1975 LWC*.

Loomis, John L., Antireflection Coating Designs for 10.6 Micron Window Materials, AFWL-TR-72-180.

Macleod, H. A., Thin Film Optical Filters, American Elsevier, New York (1969).

Muchmore, Robert B., "Optimum Band Width for Two Layer Anti-Reflection Films," *J. Opt. Soc. America*, 38, 20 (1948).

Musset, A. and A. Thelen, "Antireflection Coatings" (*Progress in Optics*) 8, 203-237 (1970).

AFML-TR-76-103

BIBLIOGRAPHY (Contd)

Optical Design, Military Standardization Handbook - 141, Sections 21, 22, and 23 (1962).

Rudisill, J., M. Braunstein, and J. Bowers, "Antireflection Coatings for  $\text{CaF}_2$  Laser Windows Operating at  $5.3 \mu\text{m}$ ", p. 329, Proc. 1975 LWC.

Sahagian, Charles S. and Carl A. Pitcha, Compendium on High Power Infrared Laser Window Materials, AFCRL-72-0170.

Thelen, Alfred, "Design of Multilayer Interference Filters," Physics of Thin Films, 5, 47-48 (1969).

Willingham, C., Bua, D., Statz, H., and Horrigan, Laser Window Studies, ARPA 1180, S-1900, Aug. 75, Contract #DAAH01-74-C-0719. (fluoride polishing and  $5\text{-}3 \mu$  coating absorption).

Willingham, C., D. Bua, T. Varitimos, M. Schapira, and H. Statz, "Laser Calorimetry of Infrared Optical Thin Films", p. 355, Proc. 1975 LWC.

Young, P. A. and W. G. Thege, "Two-Layer Laser Antireflection Coatings," J. Phys. D: Appl. Phys. 4, 64 (1971).